CANADIAN THESES

THÈSES CANADIENNES

NOTICE

The quality of this microfiche is heavily dependent upon the quality of the original thesis submitted for microfilming. Every effort has been made to ensure the highest quality of reproduction possible.

If pages are missing, contact the university which granted the degree.

Some pages may have indistinct print especially if the original pages were typed with a poor typewriter ribbon or if the university sent us an inferior photocopy.

Previously copyrighted materials (journal articles, published tests, etc.) are not filmed.

Reproduction in full or in part of this film is governed by the Canadian Copyright Act, R.S.C. 1970, c. C-30.

AVIS

La qualité de cette microfiche dépend grandement de la qualité de la thèse soumise au microfilmage. Nous avons tout fait pour assurer une qualité supérieure de reproduction.

S'il manque des pages, veuillez communiquer avec l'université qui a conféré le grade.

La qualité d'impression de certaines pages peut laisser à désirer, surtout si les pages originales ont été dactylographiées à l'aide d'un ruban usé ou si l'université nous a fait parvenir une photocopie de qualité inférieure.

Les documents qui font déjà l'objet d'un droit d'auteur (articles de revue, examens publiés, etc.) ne sont pas microfilmés.

La reproduction, même partielle, de ce microfilm est soumise à la Loi canadienne sur le droit d'auteur, SRC 1970, c. C-30.

THIS DISSERTATION HAS BEEN MICROFILMED EXACTLY AS RECEIVED

LA THÈSE A ÉTÉ MICROFILMÉE TELLE QUE NOUS L'AVONS REÇUE

A Modified Potential Method for Transonic Flow Problems

Bao Quy Nguyen

A Thesis

in

The Department

of

Mechanical Engineering

Presented in Partial Fulfillment of the Requirements
for the Degree of Master of Engineering at
Concordia University
Montréal, Québec, Canada

March 1986

ISBN 0-315-30658-0

ABSTRACT

A Modified Potential Method for Transonic Flow Problems

Bao Quy Nguyen

Transonic flows are of high interest in the design of aircraft and turbomachines. The governing equations for inviscid transonic flows are nonlinear and of mixed-type, calling for complicated numerical treatment. The classical velocity potential and stream function models are the most used formulations for such flows. They are not, however, without limitations. The potential method has been proven inapplicable for choked flows and inaccurate for flows with strong shocks. It has also recently been discovered to suffer from a multiple solutions problem. The stream function method also suffers from a double-valuedness problem in mixed flow situations.

In this Thesis, two new formulations for transonic flow problems are proposed based on a modified potential model and a hybrid model. In the first, a non-isentropic potential model is developed based on the entropy condition obtained by shock tracking or by solving a pressure equation. The second approach, called a hybrid one, is in terms of a velocity potential and a perturbation stream function. It goes one step further by accounting for the vorticity generated behind curved shocks by the entropy gradient.

The results for choked flow in a converging- diverging nozzle are shown to be unique and agree well with the analytical solution. Results over a non-lifting airfoil reproduce the features of Euler solutions.

ACKNOWLEDGEMENTS .

The author wishes to extend his thanks to his Thesis supervisor, Dr. W. G. Habashi for his continuous support and encouragement throughout the course of this research.

Thanks are also due to Dr. M. V. Bhat for providing the opportunity to complete some of the computations for this Thesis after the candidate joined the staff of Pratt & Whitney Canada. The author would like to acknowledge the valuable help and suggestions of his colleagues and friends, Messrs. P. L. Kotiuga, L. A. McLean, V. Tata and G. Guevremont. Some of the graphs were done by Mr. H. Nguyen and his help is appreciated. Technical assistance from the staff of the Computational Fluid Dynamics Laboratory at Concordia University is acknowledged.

The author is greatly indebted to his family, and also to N.P.T.N., for their unfailing support and patience during the course of this study.

The financial support of the Natural Sciences and Engineering Research Council of Canada through an NSERC Graduate Scholarship is gratefully acknowledged.

To my Mother and Father.

NOMENCLATURE

A	cross-sectional area of nozzle
a	speed of sound
E	energy
$e^{-\Delta S/R}$	entropy function across a shock
f	right-hand side vector
h	enthalpy
K	global influence matrix
k	element influence matrix
M	Mach number
m	mass flow rate
N	shape function
p	pressure
q	velocity, $\sqrt{u^2 + v^2}$
R	gas constant
Re	residual
S	entropy
T	temperature
u,v	x and y velocity components
x,y	Cartesian coordinates
W	weighting function
α, β	relaxation factors
γ	isentropic exponent
δ, Δ	change in a quantity
Φ	potential
Ψ	stream function

Ψ'	perturbation stream function
μ	artificial viscosity or artificial compressibility coefficient
ρ	density
$\tilde{\rho}$	artificial compressibility
ω	vorticity

Subscripts

e, e-1	element, upstream element
ex	exit
i,j	nodal indices
in	inlet
n	outward normal direction
o	stagnation property
s	streamwise direction
x,y,t	derivatives with respect to x, y and time
∞	freestream value

Superscripts

'(apostrophe)	isentropic value
*	non-dimensional value

TABLE OF CONTENTS

LIST OF FIGURES

CHAPTER 1
INTRODUCTION

1.1 Inviscid Transonic Flow Problem - An Overview

The motion of a general unsteady viscous compressible flow is governed by the Navier-Stokes equations, which are a system of nonlinear coupled partial differential equations. Exact solutions cannot be found except for few highly specialized cases. Aerodynamicists normally have to turn to numerical methods to obtain analytical solutions. In such cases, however, sufficient simplifications must still be made to bring the computation efforts to manageable proportions and to obtain an approximate but meaningful solution.

In the last decade, the use of such numerical methods for flow simulation has become a powerful and indispensible tool for the design and analysis of modern aircraft and turbomachines. This is mainly due to the rapid growth of computer technology as well as the development of new, accurate and efficient numerical algorithms.

Among the growth areas of computational aerodynamics, a great effort has been expended towards developing numerical algorithms for transonic flow problems. Transonic flight, now recognized as an efficient regime for aircraft, is also quite frequently encountered in turbomachinery cascade passages and has become a challenging focus of interest.

For flows with sufficiently high Reynolds numbers, the viscous effects are important only in a thin shear layer near the body surface, as suggested by Prandtl's boundary layer theory. The remainder of the flow

can be considered inviscid. This is the basis of most present transonic inviscid calculations and is the focus of this Thesis.

1.2 Governing Equations for Two-Dimensional Inviscid Flows

The governing equations for general two-dimensional inviscid compressible flows are obtained from the conservation of mass, momentum and energy. In the absence of body forces,

1.2.1 Conservation of Mass:

$$\underline{\nabla} \cdot (\rho \underline{U}) = 0 \qquad (1.1)$$

where: $\underline{\nabla} = \frac{\partial}{\partial x} i + \frac{\partial}{\partial y} j$

and: $\underline{U} = u i + v j$

1.2.2 Conservation of Momentum:

$$\rho (\underline{U} \cdot \underline{\nabla}) \underline{U} = - \underline{\nabla} p \qquad (1.2)$$

where p is the static pressure.

1.2.3 Conservation of Energy

$$\underline{\nabla} \cdot (\rho E_o \underline{U}) = - \rho (\underline{U} \cdot \underline{\nabla}) p \qquad (1.3)$$

where E_o is the total energy.

The system of equations (1.1 - 1.3) are known as the Euler equations.

This set of first-order hyperbolic equations has been vigorously tackled in the last few years by many researchers and it has become increasingly fashionable to solve the Euler equations in their "primitive" variables form.

It should be noted from the above equations that, to compute the flow field, four unknowns must be solved for: two velocity components and two thermodynamic properties. The computational requirements of the Euler equations are thus substantially higher than the more traditional velocity potential and stream function methods for which a single unknown need be determined, as will be shown in the next section.

To introduce the "single" variable methods such as the velocity potential or the stream function, the governing equations are combined and/or replaced by simpler relations.

For steady, isentropic flow of a perfect gas, the energy equation is:

$$\frac{\rho}{\rho_o} = [1 - \frac{\gamma - 1}{2} M_o^2]^{1/(\gamma-1)} \qquad (1.4)$$

where: $M_o = q/a_o$ is the Mach number with respect to the stagnation speed of sound.

From the first and second laws of thermodynamics, one has:

$$TdS = dh - \frac{dp}{\rho}$$

or: $$T\underline{\nabla}S = \underline{\nabla}h - \frac{1}{\rho}\underline{\nabla}p$$

$$= \underline{\nabla}[h_o - \frac{1}{2}\underline{\nabla}(\underline{U}\cdot\underline{U})] - \frac{1}{\rho}\underline{\nabla}p$$

The momentum equation (1.2) is now:

$$(\underline{U}\cdot\underline{\nabla})\underline{U} = \frac{1}{2}\underline{\nabla}(\underline{U}\cdot\underline{U}) - \underline{U}\times\underline{\nabla}\times\underline{U}$$

$$= T\underline{\nabla}S - \underline{\nabla}[h_o - \frac{1}{2}\underline{\nabla}(\underline{U}\cdot\underline{U})]$$

or: $$-\underline{U}\times\underline{\nabla}\times\underline{U} = T\underline{\nabla}S - \underline{\nabla}h_o \qquad (1.5)$$

By defining the vorticity vector as:

$$\underline{\omega} = \underline{\nabla}\times\underline{U} \qquad (1.6)$$

equation (1.5) becomes:

$$\underline{U}\times\underline{\omega} = -T\underline{\nabla}S + \underline{\nabla}h_o \qquad (1.7)$$

Equation (1.7) is usually known as the Crocco relation. Expressed in a natural coordinate system aligned with the flow, equation (1.7) becomes:

$$\underline{q}.\underline{\omega} = T\frac{\partial S}{\partial n} \qquad (1.8)$$

which expresses the vorticity in terms of the gradient of entropy across the

streamlines.

The governing equations are now reduced to the continuity and vorticity equations, supplemented by the Crocco relation (1.8), i.e.:

(1) The Continuity Equation:

$$\frac{\partial}{\partial x}(\rho u) + \frac{\partial}{\partial y}(\rho v) = 0 \qquad (1.9)$$

(2) The Vorticity Equation :

$$\frac{\partial u}{\partial y} - \frac{\partial v}{\partial x} = \omega \qquad (1.10)$$

with the vorticity ω given by equation (1.8).

The stream function and velocity potential formulations are based on the simplified system consisting of (1.4), (1.9), (1.10) and (1.8).

1.3 Stream Function Equation

In this approach, a stream function, Ψ, is defined to satisfy the equation of continuity identically:

$$u = \frac{1}{\rho}\frac{\partial \Psi}{\partial y} \qquad (1.11a)$$

and:

$$v = -\frac{1}{\rho}\frac{\partial \Psi}{\partial x} \qquad (1.11b)$$

The vorticity equation (1.10) then provides the governing equation in terms of the stream function:

$$\frac{\partial}{\partial x}\left(\frac{1}{\rho}\frac{\partial \Psi}{\partial x}\right) + \frac{\partial}{\partial y}\left(\frac{1}{\rho}\frac{\partial \Psi}{\partial y}\right) = -\omega \qquad (1.12)$$

The vorticity ω is given by the Crocco relation (1.8), which can be re-arranged as follows:

$$\omega = \frac{T}{q}\frac{\partial S}{\partial n}$$

$$= \frac{RT}{q}\frac{\partial}{\partial n}\left(\frac{S}{R}\right)$$

For a perfect gas, since $p = \rho RT$:

$$\omega = \frac{p}{\rho q}\frac{\partial}{\partial n}\left(\frac{S}{R}\right)$$

$$= p\frac{\partial}{\partial \Psi}\left(\frac{S}{R}\right) = \frac{a}{\gamma M}\frac{\partial}{\partial n}\left(\frac{S}{R}\right) \qquad (1.13)$$

using, in the first expression, the fact that the normal derivative of the stream function is the mass flux (ρq) between two streamlines and the definition of the speed of sound in the second.

For incompressible flows, the above equation implies that vorticity remains constant along a streamline and for compressible flows, it simply states that the vorticity/pressure ratio is constant along a streamline.

The energy equation (1.4), in terms of Ψ is:

$$\frac{\rho}{\rho_o} = \left[1 - \frac{\gamma - 1}{2} M_o^2\right]^{1/(\gamma - 1)}$$

$$= \left[1 - \frac{\gamma - 1}{2}\left(\frac{\nabla \Psi}{a_o \rho}\right)^2\right]^{1/(\gamma - 1)} \qquad (1.14)$$

It can be seen that no assumptions are made in recasting the Euler equations system into a stream function/vorticity system. It is therefore appropriate to expect that a solution of the new system of equations should yield results totally in accordance with those of the Euler system.

1.4 Velocity Potential Equation

If the flow is further assumed irrotational, the velocity can be defined as the gradient of a potential to satisfy the vorticity equation identically,

$$\underline{U} = \underline{\nabla}\,\Phi \;;\; u = \frac{\partial \Phi}{\partial x} \;\;;\;\; v = \frac{\partial \Phi}{\partial y} \tag{1.15}$$

The continuity equation then yields:

$$\frac{\partial}{\partial x}\left(\rho \frac{\partial \Phi}{\partial x}\right) + \frac{\partial}{\partial y}\left(\rho \frac{\partial \Phi}{\partial y}\right) = 0 \tag{1.16}$$

The energy equation is:

$$\frac{\rho}{\rho_o} = \left[1 - \frac{\gamma - 1}{2} M_o^2\right]^{1/(\gamma - 1)}$$

$$= \left[1 - \frac{\gamma - 1}{2}\left(\frac{\nabla \Phi}{a_o}\right)^2\right]^{1/(\gamma - 1)} \tag{1.17}$$

1.5 Difficulties of Transonic Solutions

The complexities of the potential or stream function transonic

flow formulations lie primarily in the mixed-type nature of these equations. For subsonic flows, the equations are elliptic but as the free stream velocity exceeds the critical value, a supersonic pocket develops over the body and the equations become locally hyperbolic. Furthermore, the equations accept discontinuous solutions through the formation of shock waves. Both compression and expansion shocks are, however, permitted by the equations. Expansion shocks are physically impossible and must be excluded. The limits of the supersonic regions, as well as the shock strength, are also not known *a priori* and must be determined along with the solution.

Let us now examine the solution method for inviscid transonic flows using the velocity potential formulation in order to highlight some of these points.

1.5.1 The Concept of Artificial Viscosity for the Mixed-Type Equation

The potential equation (1.16) can be rewritten in characteristic or non- conservative form as:

$$(a^2 - u^2)\Phi_{xx} - 2uv\Phi_{xy} + (a^2 - v^2)\Phi_{yy} = 0 \qquad (1.18)$$

An interesting phenomenon can be demonstrated from this equation in the transonic regime. Since the equation is symmetric it remains unchanged regardless of whether the velocity $\underline{U}$ is defined as $\underline{\nabla}\Phi$ or $-\underline{\nabla}\Phi$. This implies that the equation permits reverse flow solutions. For illustrative purposes, let us consider the flow over a symmetric biconvex airfoil, depicted in Fig. 1.1. If central differences are used everywhere, two shocks appear with one of them being a non-physical expansion shock. If

forward differences are applied for supersonic points, only an expansion shock is obtained. Only when backward differences are used for supersonic points will a compression shock appear in the solution. The use of backward differences in the supersonic regions in order to capture shocks was first made by Murman and Cole [1] for the solution of steady transonic flow over thin airfoils, using the transonic small disturbance equation. Their approach was extended to the full potential equation by Garabedian [2] and Jameson [3] and has been in wide use since.

To illustrate Jameson's approach to the full potential equation, let us recast equation (1.18) in a coordinate system locally aligned with the flow, i.e. along a streamline and the normal to it. The equation reads:

$$(1 - M^2)\,\Phi_{ss} + \Phi_{nn} = 0 \tag{1.19}$$

where the local derivatives with respect to (s,n) are defined in terms of the global derivatives with respect to (x,y) as:

$$\Phi_{ss} = (1/q^2)[u^2\Phi_{xx} + 2uv\Phi_{xy} + v^2\Phi_{yy}] \tag{1.20a}$$

and:

$$\Phi_{nn} = (1/q^2)[v^2\Phi_{xx} - 2uv\Phi_{xy} + u^2\Phi_{yy}] \tag{1.20b}$$

This method, known as the rotated differences scheme, takes into account the non-alignment of the grid and local velocity vector in representing the domain of dependence more accurately in supersonic regions.

It is obvious that equation (1.19) is elliptic for subsonic flows ($M < 1$) and hyperbolic for supersonic flows ($M > 1$). This is an important

property of the full potential equation and it is classified as being of mixed-type.

Let us, in general, consider the numerical treatment of a differential equation of the above mixed-type written in the following form:

$$A\,\Phi_{ss} + \Phi_{nn} = 0 \quad ; \quad A = 1 - M^2 \tag{1.21}$$

If upwind or backward differences in the streamwise direction are applied to discretize the Φ_{ss} term, one obtains:

$$(1 - M^2)(\Phi_i - 2\,\Phi_{i-1} + \Phi_{i-2})/\Delta s^2$$

This can be re-expressed in terms of central differences and a correction as:

$$= (1 - M^2)\,[(\Phi_{i+1} - 2\Phi_i + \Phi_{i-1}) -$$

$$(\Phi_{i+1} - 3\,\Phi_i + 3\,\Phi_{i-1} + \Phi_{i-2})]/\Delta s^2$$

$$= (1 - M^2)(\Phi_{i+1} - 2\,\Phi_i + \Phi_{i-1})\,/\Delta s^2 -$$

$$(1 - M^2)[(\Phi_{i+1} - 2\Phi_i + \Phi_{i-1}) - (\Phi_i - 2\,\Phi_{i-1} + \Phi_{i-2})]/\Delta s^2$$

$$= (1 - M^2)(\Phi_{i+1} - 2\,\Phi_i + \Phi_{i-1})\,/\Delta s^2 - (1 - M^2)\,\Delta s\,\Phi_{sss}$$

$$= (1 - M^2)(\Phi_{i+1} - 2\,\Phi_i + \Phi_{i-1})\,/\Delta s^2 + M^2(1 - 1/M^2)\,\Delta s\,u_{ss}$$

(1.22)

the correction term on the right-hand side of (1.22) is observed to be a viscous-like term, similar to the right-hand side terms in the Navier-Stokes equations and it can be concluded that the use of backward difference operator in the supersonic region introduces an "artificial viscosity" in the inviscid potential equation proportional to the grid spacing. This artificial viscosity has a switching factor defined as:

$$\mu \, \Delta s \, u_{ss} \;\; ; \;\; \mu = \max (0 \, , \, 1 - 1/M^2)$$

that limits its introduction to supersonic points.

It has been lately recognized by Hafez, Murman and South [4] that the artificial viscosity term can be absorbed in the density to produce a more compact form in the following manner: if one rewrites the upwind differences form for the components of Φ_{ss}, from (1.20a), an artificial viscosity is obtained for each component as:

$$\Phi_{xx} : \Phi_{xx} - \Delta x \Phi_{xxx}$$

$$\Phi_{xy} : \Phi_{xy} - (\Delta x/2) \, \Phi_{xxy} - (\Delta y/2) \, \Phi_{xyy}$$

$$\Phi_{yy} : \Phi_{yy} - \Delta y \, \Phi_{yyy}$$

The overall viscosity is then:

$$(1 - M^2)(1/q^2)[u^2 \Delta x \Phi_{xxx} + uv \Delta y \, \Phi_{xyy} + uv \Delta x \, \Phi_{xxy} + v^2 \Delta y \, \Phi_{yyy}]$$

$$= (1 - M^2)(1/q^2)[\Delta x(u^2 u_{xx} + uvv_{xx}) + \Delta y(uvu_{yy} + v^2 v_{yy})]$$

This, when multiplied by ρ, can be shown [5] to be equivalent to:

$$-(1 - 1/M^2)\ [(u\rho_x)_x \Delta x + (v\rho_y)_y \Delta y]$$

Equation (1.18) can now be recast as:

$$(\rho u)_x + (\rho v)_y = [(1 - 1/M^2)\, u\rho_x \Delta x]_x + [(1 - 1/M^2)\, v\rho_y \Delta y]_y \qquad (1.23)$$

or:
$$(\rho_1 \Phi_x)_x + (\rho_2 \Phi_y)_y = 0 \qquad (1.24)$$

where:
$$\rho_1 = \rho - \max\,[0,(1 - 1/M^2)]\ u\ \rho_x \Delta x$$

and:
$$\rho_2 = \rho - \max\,[0,(1 - 1/M^2)]\ v\ \rho_y \Delta y$$

A simpler, approximate form of (1.23) is given by:

$$(\tilde{\rho}\, \Phi_x)_x + (\tilde{\rho}\, \Phi_y)_y = 0 \qquad (1.25)$$

where ρ is the artificial compressibility and is given by:

$$\tilde{\rho} \approx \rho - \mu \rho_s \Delta s \qquad (1.26)$$

$$\rho_s \Delta s = (u/q)\, \rho_x \Delta x + (v/q)\, \rho_y \Delta y \qquad (1.27)$$

and: $\mu = \max\ (0\ ,\ 1 - 1/M^2)$ (1.28)

is a switching function vanishing in the subsonic region.

The above approach, which was proposed by Hafez et al [4], is commonly known as the Artificial Compressibility Method (ACM). It proved to be a breakthrough for transonic flow calculations especially for the finite element method, and is now widely used due to its simplicity and ease of implementation. Results using the full potential equation with the ACM can be found in Refs.[6 - 9].

1.5.2 Non-Uniqueness of the Potential Solution

While the full potential equation with artificial viscosity has enjoyed wide use in transonic flow computations, it has recently been found to suffer from a non-uniqueness problem. Steinhoff and Jameson [10] and later Salas *et al* [11] reported that, for a certain class of problems, multiple solutions may be produced by the potential equation in conservation form, satisfying identical boundary conditions and permitting only compression shocks. They concluded that this non-uniqueness is an inherent problem and since this is not related to the physical phenomenon, the theory of potential flow in the transonic range should be reviewed for its validity [11].

Several successful attempts have been made, since, to modify the potential formulation to account for the entropy rise across the shock and to circumvent the non-uniqueness problem. Hafez and Lovell [12], for instance, proposed a non-isentropic potential model where the entropy jump is accounted for. Another approach is provided by Habashi, Hafez and Kotiuga [13], who solve a pressure equation derived from the momentum equations, in conjunction with the potential equation, and calculate an

entropy correction determined by the deviation of the calculated pressure from the isentropic one. Both approaches will be covered in Chapter 2. The point to be made here, however, is that one should not let the so-called non-uniqueness problem detract from the many obvious advantages of the potential formulation.

1.5.3 Inapplicability of the Potential Solution to Internal Flows with Shocks

For an internal flow such as the flow in a convergent-divergent nozzle the back pressure may lead to a situation where the nozzle is choked and a shock appears past the throat. The shock positions itself to create the appropriate loss in total pressure to meet the imposed back pressure. By virtue of the fact that the potential model is an isentropic one, it is impossible to meet a back pressure other than the isentropic one. This led many researchers to conclude that, for internal transonic flows, the Euler equations were the only suitable method of solution. By analyzing the problem and its boundary conditions, however, one comes to the conclusion, as will be shown in Chapter 2, that minor modifications of the potential flow formulation allow it to be successfully extended to choked internal flows with shocks.

1.5.4 Transonic Stream Function Equation

The advantages of the Ψ formulation over the Euler equations are many. Let us, however, mention two important ones, (a) the solution of a one variable problem versus four variables, (b) the solution of a second-order equation rather than a set of first-order equations with complicated boundary conditions. The obvious advantage of the Ψ

formulation over the full potential method is its ability to include the rotational effects due to entropy gradients behind a curved shock and to its simpler Dirichlet boundary conditions. Unfortunately, the model contains a classical difficulty for mixed subsonic/supersonic flows: the double-valuedness of the density-mass flux relation, as illustrated in Fig. 1.2. For a particular value of mass flux (ρq), two values of density can be determined, one corresponding to a subsonic Mach number and the other to a supersonic one.

This singularity has been remedied in [14] by alternatively iterating between the stream function equation and the same equation recast in terms of the velocity q, once the stream function distribution (hence the flow orientation) is known:

$$\theta = \tan^{-1}\left(\frac{v}{u}\right) = \tan^{-1}\left(\frac{\rho v}{\rho u}\right) = \tan^{-1}\left(-\frac{\Psi_x}{\Psi_y}\right) \qquad (1.29)$$

The vorticity equation becomes:

$$\frac{\partial u}{\partial y} - \frac{\partial v}{\partial x} \equiv \frac{\partial}{\partial y}(q\cos\theta) - \frac{\partial}{\partial x}(q\sin\theta) = -\omega \qquad (1.30)$$

where: $q = \sqrt{(u^2 + v^2)}$

Equation (1.30) is first-order in terms of q and can be integrated if a solution is known along an initial data line other than a characteristic. For flows over isolated airfoils, for example, the initial data line is usually the far field boundary representing the free stream. The equation is then integrated in the general direction of its characteristic. Results using the stream function formulation can be found, for instance, in

[14] and [15] showing the effect of vorticity in displacing the shock position upstream compared with those given by the irrotational velocity potential model.

1:6 Summary

The transonic flow problem with its physical and theoretical difficulties has been simulated to a considerable degree of success for the last decade. Since the first solutions in the early 70's, based on the simple model of small perturbations, aerodynamicists have now developed powerful tools to predict and analyse flow phenomena which previously could only be observed experimentally.

The potential equation has proved to be a powerful and reliable method to predict transonic inviscid flows despite its few perceived limitations. The major constraint of the potential assumption is that the rotational effects are ignored making it somewhat inaccurate for curved shocks. While the anomaly of multiple solutions and the internal flow difficulties have brought the applicability of the full potential solutions under close scrutiny, the newly developed modified formulations would probably remain among the best methods for the numerical solution of the transonic problem and continue to serve computational transonics well.

The stream function formulation offers a higher approximation of transonic inviscid flows than the potential model since the rotational effects are faithfully reflected. The inclusion of vorticity should yield more realistic results in the presence of strong shocks.

1.7 Scope of Thesis

Two new formulations for the transonic flow problem are proposed and are based on a modified potential model.

In the first approach, called the Modified Potential Method, only the entropy jump is accounted for, while in the second approach, or the Hybrid Method, both the entropy and vorticity are calculated.

In the next chapter, the derivation of the governing equations with the modified potential and hybrid potential/stream function models are presented, together with their discretization using the finite element method. Some iterative schemes appropriate for transonic solutions are illustrated in Chapter 3. Results and discussion are presented in the last chapter.

CHAPTER 2
PROBLEM FORMULATION

In this chapter, the two approaches based on a modified potential and a hybrid potential/stream function are demonstrated. The methods are applied to the analysis of both internal and external transonic flows.

Choked internal flows are used to illustrate the modified potential method and it compares favorably with the exact solution for one-dimensional flow. The hybrid method applied to non-lifting airfoils shows the trends of an Euler solution, at a fraction of the cost.

The finite element analysis is presented in the following section with special emphasis on the ease of application of some particularly problematic boundary conditions.

2.1 Assumptions

In deriving the governing equations in the subsequent sections, the flow is assumed to be isentropic and irrotational up to the shock wave. Downstream of the shock, the ratio (entropy/pressure) remains constant along the streamlines but the entropy gradient across the streamlines causes vorticity.

The flow stagnation properties may be determined by the isentropic relations before the shock. Although the flow becomes rotational thereafter, these properties can be found, along each streamline, by the same relations modified by the correct entropy increase.

2.2 Mathematical Model

As mentioned in Chapter 1, the transonic potential equation is not adequate to simulate flows in some cases. For low transonic cases where shocks are weak the isentropic assumption does not produce a significant error and the potential equation results are acceptable. As the free stream Mach number increases, and the shock strengthens, the potential model becomes less accurate since the flow can no longer be regarded as isentropic. Another serious problem of the potential formulation is the non-unique solutions in a certain range of free stream Mach numbers for external flows, while for internal flows the isentropic potential solution may not exist at all.

In the present Thesis, two new approaches are suggested to modify the potential model in order to include the non-isentropic and/or rotational effects.

2.3 One-Dimensional Flow

For the one-dimensional internal flow example, let us consider a compressible flow in a converging-diverging nozzle as described in Ref. [17].

2.3.1 Non-Uniqueness of the Classical Potential Solution for Choked Flows

The continuity equation can be solved analytically to yield two isentropic solutions with a sonic point at the throat as shown in Fig. 2.1. For subsonic inlet conditions, the flow expands in the converging part and compresses in the diverging part of the nozzle. If the sonic condition is

reached at the throat, two cases are possible: (i) the flow may continue compressing following the subsonic solution (curve B) or (ii) the flow may expand to supersonic conditions (curve A) and jump to a subsonic solution through the formation of a normal shock in the diverging section. In both cases, the solution is controlled by the exit pressure, which in general does not correspond to the isentropic pressure.

The shock position can be uniquely determined only if the pressure loss or the entropy increase is taken into account. The classical isentropic potential solution simply does not exist in this case [14].

Habashi et al, in Ref. [14], show that a Neumann boundary condition for the potential at the exit produces non-unique solution for the choked nozzle.

Consider the one-dimensional equation:

$$[\Phi_x^2]_x = 0 \qquad (2.1)$$

for $0 \leq x \leq L$. For subsonic inflow, the inlet boundary condition is:

$$x = 0 \; ; \; \Phi = 0$$

At the exit, where the flow becomes subsonic again due to the presence of a normal shock in the nozzle, one can impose either of the followings:

$$x = L \; ; \; \Phi_x = C_1 \text{ or } \Phi = C_2$$

Upon integrating equation (2.1), one can write:

$$\Phi_x^2 = C_3^2$$

or: $$\Phi_x = \pm C_3$$

From the upstream conditions, one has:

$$\Phi_x = +C_3$$

and if the Neumann condition at the exit is selected:

$$\Phi_x = C_1 = -C_3$$

which implies that the solution cannot be uniquely determined, as illustrated in Fig. 2.2.

Now, if the Dirichlet condition, $\Phi = C_2$ is chosen, the shock location is given by [14]:

$$x_s = L - [\Phi(x_s) - C_2]/C_1 \qquad (2.2)$$

where: $\Phi(x_s)$ is the potential value at x_s.

2.3.2 The Modified Potential Method - Model 1

Having recognized the boundary difficulty that hindered the solution of choked flows, Habashi, Hafez and Kotiuga [13] and Deconinck and Hirsch [18] developed potential flow methods capable of solving internal flow with shocks. The former approach is more general and is based on a modified potential formulation in which the entropy increase across the

shock is taken into account via the Rankine-Hugoniot relation.

Since vorticity cannot exist in the one-dimensional case, even in the presence of shocks, the velocity can be defined as the gradient of a potential, i.e.:

$$u = \Phi_x \tag{2.3}$$

The continuity equation is:

$$[\rho A u]_x = 0 \tag{2.4}$$

which can be written in terms of the potential as:

$$[\rho A \Phi_x]_x = 0 \tag{2.5}$$

The density ρ is a function of u and is obtained from the following modified expression:

$$\frac{\rho}{\rho_o} = [1 - \frac{\gamma - 1}{2} M_o^2]^{1/(\gamma - 1)} \cdot e^{-\Delta S/R} \tag{2.6}$$

where the term $e^{-\Delta S/R}$ is unity before the normal shock while after the shock, the entropy jump is given by the Rankine-Hugoniot relation:

$$\Delta S/R = \ln [(\frac{2\gamma M_s^2}{\gamma + 1} - \frac{\gamma - 1}{\gamma + 1})^{1/\gamma - 1} / (\frac{(\gamma + 1) M_s^2}{2 + (\gamma - 1) M_s^2})^{\gamma/\gamma - 1}] \tag{2.7}$$

2.3.3 Boundary Conditions

At the inlet (x = 0),

$$\Phi(x=0) = 0 \tag{2.8}$$

for subsonic inflow conditions.

A Dirichlet boundary condition must be imposed at the nozzle exit in order to uniquely define the shock location:

$$\Phi(x=L) = C_3 \tag{2.9}$$

The value of C_3 can be varied to adjust the shock position, and hence its strength, in the diverging section of the nozzle to produce the correct exit pressure. In our solution, the value of C_3 is obtained iteratively.

2.3.4 The Modified Potential Method - Model 2

An alternative way to calculate the losses in an automatic manner is to solve for the pressure determined from a second-order differential equation derived from the two momentum equations. This pressure then yields the losses and permits the calculation of the correct density [19].

The continuity equation is:

$$(\rho \Phi_x A)_x = 0 \tag{2.5}$$

While the momentum equation for the one-dimensional case can be written as:

$$(A \rho u^2)_x - A p_x = 0 \qquad (2.10)$$

This equation is turned into a second-order equation suitable for solution by finite elements by differentiating it with respect to x:

$$(A \rho u^2)_{xx} - (A p_x)_x = 0 \qquad (2.11)$$

2.3.5 Boundary Conditions

The boundary conditions for the potential equation (2.5) remain as before while those for the second-order momentum equation are as follows:

(a) at inlet (x = 0), the pressure gradient is specified from the original first order equation:

$$p_x = (A\rho u^2)_x / A \qquad (2.12)$$

(b) at exit (x = L), the static pressure is prescribed, i.e. a Dirichlet boundary condition is imposed:

$$p = p_{ex} \qquad (2.13)$$

These boundary conditions are summarized in Fig. 2.3.

Once the pressure field is determined, the losses can be found as :

$$P_L = p/p' \equiv e^{-\Delta S/R} \qquad (2.14)$$

where the prime denotes the ideal isentropic value defined from:

$$\frac{p'}{p_o} = [1 - \frac{\gamma - 1}{2} M_o^2]^{\gamma/(\gamma-1)} \qquad (2.15)$$

and the non-isentropic density is calculated as :

$$\frac{\rho}{\rho_o} = [1 - \frac{\gamma - 1}{2} M_o^2]^{1/(\gamma-1)} \cdot e^{-\Delta S/R} \qquad (2.6)$$

While the proposed method involves the solution of an additional equation, namely a Poisson equation for pressure, its results are thought to be much closer to the solution of the Euler equations, still at a fraction of the cost.

2.4 Two-Dimensional Flow

The above approaches can be easily extended to the two-dimensional case as demonstrated in Hafez, Habashi and Kotiuga [19]. However, another approach will be considered here to offer a second alternative.

The velocity components can be redefined, without any loss of generality, as a combination of the gradient of a potential and the curl of a divergence free term:

$$u = \frac{\partial \Phi}{\partial x} + \frac{1}{\rho} \frac{\partial \Psi'}{\partial y} \qquad (2.16a)$$

$$v = \frac{\partial \Phi}{\partial y} - \frac{1}{\rho} \frac{\partial \Psi'}{\partial x} \qquad (2.16b)$$

Note that the correction terms are chosen based on a stream function-like concept and for the remaining of this work, Ψ' is referred to

as the perturbation stream function.

As an example of a two-dimensional flow, let us consider the unbounded flow around a symmetric non-lifting airfoil.

2.4.1 Governing Equations

By substituting the definition of the velocity given in (2.16a,b) in the continuity and vorticity equations, one obtains:

$$\frac{\partial}{\partial x}\left(\rho \frac{\partial \Phi}{\partial x}\right) + \frac{\partial}{\partial y}\left(\rho \frac{\partial \Phi}{\partial y}\right) = 0 \qquad (2.17)$$

and:

$$\frac{\partial}{\partial x}\left(\frac{1}{\rho} \frac{\partial \Psi'}{\partial x}\right) + \frac{\partial}{\partial y}\left(\frac{1}{\rho} \frac{\partial \Psi'}{\partial y}\right) = -\omega \qquad (2.18)$$

The non-isentropic density is obtained from (2.6):

$$\frac{\rho}{\rho_o} = \left[1 - \frac{\gamma - 1}{2} M_o^2\right]^{-1/(\gamma - 1)} \cdot e^{-\Delta S/R} \qquad (2.6)$$

while ω is obtained from the Crocco relation (1.13).

$$\omega = \frac{a}{\gamma M} \frac{\partial}{\partial n}\left(\frac{S}{R}\right) \qquad (2.19)$$

Equations (2.17) to (2.19) constitute a set of equations governing the motion of an inviscid non-isentropic compressible flow in terms of the new variables Φ and Ψ'.

2.4.2 Boundary Conditions

The flow configuration is shown in Fig. 2.4. In order to determine the proper boundary conditions, let us consider the velocity components in terms of the two variables Φ and Ψ' along the outer boundaries and on the airfoil surface.

(a) In the far field region where the presence of the airfoil is not felt, the flow variables assume the free stream values, which are denoted by the subscript ∞. Along the outer boundaries ∂R_1, the velocity is thus:

$$\underline{U} = U_\infty$$

which implies: $u = U_\infty \quad ; \quad v = 0$

Now since the flow in the far field is irrotational and no perturbation term should be present, the boundary conditions for Φ along ∂R_1 can be taken from the potential model, i.e.:

$$\Phi = U_\infty x \tag{2.20}$$

This means that a Neumann condition should be imposed on the perturbation stream function:

$$\Psi'_n = 0 \tag{2.21}$$

(ii) On the airfoil surface, the flow tangency must be enforced. This is equivalent to setting the normal mass flux to zero along ∂R_2, or:

$$\Phi_n = 0 \tag{2.22}$$

leading to: $\Psi'_s = 0 \quad ; \quad \text{or} \quad \Psi' = \text{const.}$ (2.23)

The solution is determined to within some arbitrary constant of the variables Φ and Ψ', and the constant can be chosen as zero for

simplicity.

Since the flow should be symmetric about the centerline for this particular configuration, the stream function assumes a zero value along this line, including the slit behind the airfoil, i.e.

$$\Psi' = 0$$

along AB in Fig. 2.3.

2.5 Finite Element Discretization

The finite element discretization of the governing equations for both the one-dimensional and two-dimensional problems will be presented in this section.

2.5.1 The Galerkin Weighted Residual Method

Given a differential equation of the form:

$$L(u) = f \tag{2.24}$$

the weighted residual method seeks an approximate solution in the form of a finite number of basis functions:

$$\underline{u} = \sum_{i=1}^{n} u_i N_i(x,y) \tag{2.25}$$

where u_i are the undetermined coefficients and N_i are known as the basis or interpolation functions.

Since the approximation solution $\underline{u}$ will not, in general, satisfy the governing equation exactly, substitution of equation (2.25) into (2.24) should yield an error or a residual R, that is:

$$L(\underline{u}) - f = R \tag{2.26}$$

The main objective of the weighted residual method is to determine the coefficients u_i such that the residual R is minimized over the solution domain in an average manner. This is achieved by setting the weighted average error to zero, or:

$$\iint_A [\, L(\underline{u}) - f \,] W_i \, dxdy = 0 \tag{2.27}$$

where W_i are weighting functions which, in general, are not the same as the interpolation functions N_i. The Galerkin method, however, selects the weighting functions to be the basis functions N_i so that:

$$\iint_A [\, L(\underline{u}) - f \,] N_i \, dxdy = 0 \tag{2.28}$$

The finite element method can be formulated applying the Galerkin weighted residual method by breaking the integral (2.27) into its sum over all elements:

$$\sum_{i=1}^{NEL} \iint [\, L(\underline{u}) - f \,] N_i \, dxdy = 0 \tag{2.29}$$

2.5.2 Isoparametric Elements

One of the advantages of the finite element method is its ability

to approximate intricate boundaries. This can be achieved by a local transformation to map a distorted element into a regular-shaped parent element as shown in Fig. 2.5. Within an element, the function and the coordinates (x,y) can be expressed as:

$$f = \sum_{i=1}^{DOF} M_i(\xi, \eta)\, f_i \qquad (2.30)$$

$$x = \sum N_i(\xi, \eta)\, x_i \; ; \; y = \sum N_i(\xi, \eta)\, y_i$$

where DOF is the number of degrees of freedom, (ξ, η) are the non-dimensional coordinates of the parent or undistorted finite element and (x_i,y_i) denotes the physical coordinates of node i.

Several types of elements can be defined based on the choice of polynomials for the geometric interpolation function N_i and for the field interpolation function M_i. If the two polynomials are of the same order, the elements are called isoparametric. In contrast to the isoparametric concept, the order of M_i can be chosen to be lower or greater than that of N_i for subparametric or superparametric elements, respectively.

For four-node isoparametric bilinear elements, the shape functions are found to be:

$$N_i(\xi, \eta) = -(1 + \xi\xi_i)(1 + \eta\,\eta_i) \qquad (2.31)$$

where (ξ_i,η_i) are the coordinates of the corner node i. The shape function N_i can be observed to assume a value of unity at the corner node i and vary linearly with ξ and η along an element side $(\xi, \eta = \pm 1)$.

2.5.3 One-Dimensional Equations

By applying the Galerkin criterion to equation (2.4), one can write:

$$\sum_{i=1}^{NEL} \int_0^L N_i \frac{d}{dx}\left[\rho A \frac{d\Phi}{dx}\right] dx = 0 \qquad (2.32)$$

This can be integrated by parts to give:

$$\sum_{i=1}^{NEL} -\int_0^L \frac{dN_i}{dx}\left[\rho A \frac{d\Phi}{dx}\right] dx + \rho A \frac{d\Phi}{dx} N_i \Big|_0^L = 0 \qquad (2.33)$$

From equation (2.30), one can write:

$$\frac{d\Phi}{dx} = \sum_{i=1}^{DOF} \frac{dN_i}{dx} \Phi_i \qquad (2.34)$$

Substituting (2.34) into (2.33):

$$\sum_{i=1}^{NEL} \int_0^L \frac{dN_i}{dx}\left[\rho A \frac{dN_j}{dx}\right] dx \{\Phi_j\} = \rho A \frac{d\Phi}{dx} N_i \Big|_0^L \qquad (2.35)$$

where the repeated subscript denotes summation.

Note that the right-hand side term of (2.35) is nonzero for elements with nodes on the domain boundaries where a derivative boundary condition is prescribed. Therefore it vanishes in the present problem.

If density is assumed constant within an element, equation (2.35) can be recast as:

$$\sum_{i=1}^{NEL} \rho_e \int_0^L \frac{dN_i}{dx}\left[A \frac{dN_j}{dx}\right] dx \{\Phi_j\} = \rho_e A \frac{d\Phi}{dx} N_i \Big|_0^L \qquad (2.36)$$

or, in matrix notation:

$$[K_\Phi]\{\Phi\} = \{F_\Phi\} \tag{2.37}$$

For two-node linear elements, the element stiffness matrix $[k_\Phi]$ can be evaluated to be:

$$k_{\Phi,ij} = \rho_e \int_0^L \frac{\Delta}{L^2}\, dx\ (-1)^{i+j} \tag{2.38}$$

while the right-hand side vector is zero throughout:

$$f_{\Phi,i} = 0 \tag{2.39}$$

Similarly for the momentum equation (2.11), one can write the Galerkin formulation as:

$$\sum_{i=1}^{NEL} \int_0^L N_i\, [(A\rho u^2)_{xx} + (Ap_x)_x]\, dx = 0 \tag{2.40}$$

which, upon integration by parts, yields:

$$\sum_{i=1}^{NEL} \int_0^L A\, \frac{dN_i}{dx}\, \frac{dN_j}{dx}\, \{p_j\}\, dx = N_i\{(\rho u^2 A)_x + Ap_x\}\Big|_0^L - \int_0^L \frac{dN_i}{dx}\, (\rho u^2 A)_x\, dx \tag{2.41}$$

or, in matrix notation:

$$[K_p]\{p\} = \{F_p\}$$

$$k_{p,ij} = \int_0^L \frac{A}{L^2}\, dx\, (-1)^{i+j} \qquad (2.42)$$

and:

$$f_{p,i} = -\int_L \frac{dN_i}{dx}\frac{dN_j}{dx} \{\rho u^2 A\}_j\, dx \qquad (2.43)$$

It is observed from equation (2.41) that the first-order momentum equation appears in the boundary term, making the contour integral vanish identically. Therefore, the boundary terms need never be considered. Had the finite difference method been used, the pressure would have had to be calculated at the inlet via the first-order momentum equation. This approach, first presented here, has been extended by Hafez, Habashi and Kotiuga [19] and by Peeters, Habashi and Dueck [20] to the solution of pressure equations of both inviscid and viscous two-dimensional flows.

In the present solution, a staggered computational grid for the pressure and the potential equations is adopted, as shown in Fig. 2.6. The reason for this choice is that the momentum equation will be satisfied identically at the actual nozzle inlet.

By assembling equations (2.38), (2.39) and (2.43) for all elements, tridiagonal systems in terms of the potential Φ and pressure p result.

2.5.4 Two-Dimensional Equations

In this section, the derivation of the element equations is demonstrated for the continuity equation (2.17) while only the final expressions for the vorticity equation (2.18) are shown.

The Galerkin formulation for equation (2.17) is:

$$\sum_{i=1}^{NEL} \iint_{A_e} \left[\frac{\partial}{\partial x}\left(\rho \frac{\partial \Phi}{\partial x}\right) + \frac{\partial}{\partial y}\left(\rho \frac{\partial \Phi}{\partial y}\right) \right] N_i \, dxdy = 0 \qquad (2.44)$$

By applying Green's theorem:

$$\iint_{\Omega} u.\nabla v \, dA = \oint u(v.n)ds - \iint v.\nabla u \, dA \qquad (2.45)$$

to integrate (2.44) by parts, one obtains:

$$-\iint_{A_e} \left[\rho \frac{\partial \Phi}{\partial x}\frac{\partial N_i}{\partial x} + \rho \frac{\partial \Phi}{\partial y}\frac{\partial N_i}{\partial y}\right] dxdy + \oint N_i \rho \frac{\partial \Phi}{\partial n} ds = 0 \qquad (2.46)$$

Substituting the derivatives for Φ given by (2.34) into (2.46) to get:

$$-\iint_{A_e} \left[\rho \frac{\partial N_i}{\partial x}\frac{\partial N_j}{\partial x} + \rho \frac{\partial N_i}{\partial y}\frac{\partial N_j}{\partial y}\right] dxdy\{\Phi_j\} + \oint N_i \rho \frac{\partial \Phi}{\partial n} ds = 0 \qquad (2.47)$$

By assuming constant density over the element, one can finally write:

$$-\rho_e \iint_{A_e} \left[\frac{\partial N_i}{\partial x}\frac{\partial N_j}{\partial x} + \frac{\partial N_i}{\partial y}\frac{\partial N_j}{\partial y}\right] dxdy\{\Phi_j\} + \oint N_i \rho \frac{\partial \Phi}{\partial n} ds = 0 \qquad (2.48)$$

After assembly, equation (2.48) becomes:

$$[K_\Phi]\{\Phi\} = \{F_\Phi\} \qquad (2.49)$$

where $[k_\Phi]$ is an influence matrix of order (4 x 4) with elements:

$$k_{\Phi,ij} = \rho_e \iint_{A_e} \left[\frac{\partial N_i}{\partial x}\frac{\partial N_j}{\partial x} + \frac{\partial N_i}{\partial y}\frac{\partial N_j}{\partial y}\right] dxdy \qquad (2.50)$$

and:

$$f_{\Phi,i} = \oint \rho_e N_i \frac{\partial \Phi}{\partial n} ds \qquad (2.51)$$

Note that the contour integral (2.51) exists only for non-zero flux conditions imposed on the elements along the (global) inner and outer boundaries. Along any edge shared by two elements, the contour integral cancels. In other words, the zero flux or Neumann-type boundary conditions are naturally satisfied by the finite element method. More important in the case of the pressure equation is the fact that the two-dimensional momentum equations are naturally satisfied along the now more complex 2-D boundaries, including solid ones. Alternative formulations would have to somehow compute the pressure along the boundaries as is the case for the primitive variables Euler equations.

The vorticity equation can be discretized in the same manner:

$$\sum_{i=1}^{NEL} \iint_{A_e} \left[\frac{\partial}{\partial x}\left(\frac{1}{\rho}\frac{\partial \Psi'}{\partial x}\right) + \frac{\partial}{\partial y}\left(\frac{1}{\rho}\frac{\partial \Psi'}{\partial y}\right) + \omega\right] N_i \, dxdy = 0 \qquad (2.52)$$

which upon integration by parts yields at the element level:

$$-\left(\frac{1}{\rho_e}\right)\iint_{A_e} \left[\frac{\partial N_i}{\partial x}\frac{\partial N_j}{\partial x} + \frac{\partial N_i}{\partial y}\frac{\partial N_j}{\partial y}\right] dxdy \{\Psi'_j\} + \oint \frac{N_i}{\rho_e}\frac{\partial \Psi'}{\partial n} ds + \iint_{A_e} \omega N_i dxdy = 0 \qquad (2.53)$$

The influence matrix therefore is:

$$k_{\Psi,ij} = \left(\frac{1}{\rho_e A_e}\right) \iint \left[\frac{\partial N_i}{\partial x}\frac{\partial N_j}{\partial x} + \frac{\partial N_i}{\partial y}\frac{\partial N_j}{\partial y}\right] dxdy \qquad (2.54)$$

and the right-hand side vector is:

$$f_{\Psi,i} = \oint \left(\frac{1}{A_e \rho_e}\right) N_i \frac{\partial \Psi}{\partial n} ds + \iint N_i N_j \{\omega_j\} dxdy \qquad (2.55)$$

The derivatives in (2.50 - 2.55) are evaluated numerically:

$$\begin{bmatrix} \frac{\partial N_i}{\partial \xi} \\ \frac{\partial N_i}{\partial \eta} \end{bmatrix} = \begin{bmatrix} \frac{\partial x}{\partial \xi} & \frac{\partial y}{\partial \xi} \\ \frac{\partial x}{\partial \eta} & \frac{\partial y}{\partial \eta} \end{bmatrix} \begin{bmatrix} \frac{\partial N_i}{\partial x} \\ \frac{\partial N_i}{\partial y} \end{bmatrix} = [J] \begin{bmatrix} \frac{\partial N_i}{\partial x} \\ \frac{\partial N_i}{\partial y} \end{bmatrix} \qquad (2.56)$$

where: $\frac{\partial x}{\partial \xi} = \sum_{i=1}^{DOF} \frac{\partial N_i}{\partial \xi} x_i$

and: $[J]$: Jacobian of the transformation

The global derivatives are thus:

$$\begin{bmatrix} \frac{\partial N_i}{\partial x} \\ \frac{\partial N_i}{\partial y} \end{bmatrix} = [J]^{-1} \begin{bmatrix} \frac{\partial N_i}{\partial \xi} \\ \frac{\partial N_i}{\partial \eta} \end{bmatrix} \qquad (2.57)$$

The integrals in (2.50) and (2.54) can be determined by employing the Gaussian quadrature technique with (2 x 2) integration points [21]:

$$k = \int_{-1}^{1}\int_{-1}^{1} F(\xi,\eta)\,|J|\,d\xi\,d\eta = \sum_{i=1}^{NG}\sum_{j=1}^{NG} W_i W_j\, F(\xi_i,\eta_j)|J(\xi_i,\eta_j)| \qquad (2.58)$$

where: NG is the order of integration

W_i, W_j are the weight factors

(ξ_i , η_j) are local coordinates of the Gauss integration points.

Upon assembly of the element equations for the entire field with the assumption that density and vorticity are frozen from the previous iteration step and therefore known, two systems of simultaneous linear equations in terms of the potential and perturbation stream function are obtained. Several iterative techniques suitable for transonic problems shall be presented in the next chapter.

2.6 Artificial Compressibility Method for Finite Element Discretization

The finite element discretization shown above is not dissipative. In order to capture the correct shock, an artificial viscosity is required. In all calculations, a modified density is used at supersonic points and given by:

$$\tilde{\rho}_e = \rho_e - \mu_e \rho_s \Delta s \tag{2.59}$$

where:
$$\rho_s \Delta s \approx \rho_e - \rho_{e-1} \tag{2.60}$$

and:
$$\mu_e = \max (0 , 1 - 1/M_e^2) \tag{2.61}$$

with subscript e denoting the value at the centroid of an element e and (e-1) the value traced back along a streamline to the element upstream.

It is worth noting that in earlier finite element results using the

artificial approach, the switching function μ_e is normally amplified by a factor ranging from M^2 to $2M^2$ in order to stabilize the iterative scheme and to avoid "peaky" shocks. This leads to weaker shocks positioning farther upstream than the finite difference results which use lower artificial viscosity. Habashi and Hafez [9] propose a switching function given by:

$$\mu_e = \max (0 , 1 - 1/M_e^2 , 1 - 1/M_{e-1}^2) \qquad (2.62)$$

This helps provide unsmeared transonic results free of pre-shock accelerations. It has been actually found quite feliable for the solution stability and has been adopted by many others, for example [16].

CHAPTER 3
ITERATIVE TECHNIQUES

As can be observed in Chapter 2, the governing equations are nonlinear partial differential equations whose solutions can only be found by numerical iteration, after discretization. In this chapter, some appropriate iterative techniques for transonic solutions will be presented.

After assembling the element equations for the entire field, a system of simultaneous linear equations is formed:

$$[K]\{\Phi\} = \{f\} \tag{3.1}$$

where [K] is a symmetric sparse matrix. For the potential and stream function equations, [K] is a function of the density which is lagging behind the solution iteration-wise. In this case, the system always looks elliptic since the artificial compressibility is positive in both subsonic and supersonic regions [4]. This linearized scheme, however, will not converge for transonic flow problems. The divergence of such a scheme can be attributed to the essential nonlinearity of the governing equations which is not truthfully reflected by the matrix. For moderate to high transonic cases, the global influence matrix may become ill-conditioned.

It should also be mentioned that the numerical scheme must be carefully selected considering that for stable solutions to be obtained the numerical stencil must, at least, contain the domain of dependence of the differential equation. For elliptic equations, an explicit numerical approximation, such as the point Jacobi, can be applied to obtain the solution at a

particular grid point based on the values of the neighboring points. Now for transonic flows, as the local Mach number approaches unity, the governing equation becomes parabolic and the characteristics are normal to the streamlines. In this case, all explicit solution schemes are inapplicable and, at least, a line-implicit scheme such as Vertical Line Successive Over-Relaxation (VLSOR) must be employed.

3.1 Line Solvers

3.1.1 Vertical Line Successive Over-Relaxation (VLSOR)

The method is applied marching line by line with the flow, making use of the most recent solution of the previous line and that of the next line as boundary conditions. The resulting influence matrix is tridiagonal and the solution is relaxed in the following fashion:

$$[T]\{\delta\Phi_j^{n+1}\} = -\{Re(\delta\Phi_{j-1}^{n+1}, \Phi_{j+1}^{n})\} \qquad (3.2)$$

The over-relaxation scheme can be shown to introduce transient terms to the iteration and is recast in the time-dependent form [4].

Let us illustrate this by considering the incompressible potential equation:

$$\Phi_{xx} + \Phi_{yy} = 0 \qquad (3.3)$$

The over-relaxation solution at a particular point (i,j) is:

$$\Phi_{ij}^{n+1} = \Phi_{ij}^{n} + \alpha(\Phi^{*}_{ij} - \Phi_{ij}^{n})$$

where Φ^* is the calculated value and Φ the over-relaxed value.

The discretized equation can be rewritten as:

$$(\Phi^n_{i+1,j} - 2\Phi^*_{ij} + \Phi^{n+1}_{i-1,j})/\Delta x^2 + (\Phi^*_{i,j+1} - 2\Phi^*_{ij} + \Phi^*_{i,j-1})/\Delta y^2 = 0$$

But:

$$\Phi = (\Phi^{n+1} - \Phi^n)/\alpha + \Phi^n = \delta\Phi/\alpha + \Phi^n$$

and equation (3.3) now becomes:

$$(\Phi_{i+1,j} - 2\Phi_{ij} + \Phi_{i-1,j})^n/\Delta x^2 - 2\delta\Phi_{ij}/(\omega\Delta x^2) + \delta\Phi_{i-1,j}/\Delta x^2$$

$$+ (\Phi_{i,j+1} - 2\Phi_{ij} + \Phi_{i,j-1})^n/\Delta y^2 + (\delta\Phi_{i,j+1} - 2\delta\Phi_{ij} + \delta\Phi_{i,j-1})/(\omega\Delta y^2) = 0$$

This is equivalent to:

$$(\Phi_{xx} + \Phi_{yy})^n - (2/\alpha\Delta x^2)\delta\Phi_{ij} + (\delta\Phi_{i-1,j} - \delta\Phi_{ij} + \delta\Phi_{ij})/\Delta x^2$$

$$+ (\delta\Phi_{i,j+1} - 2\delta\Phi_{ij} + \delta\Phi_{i,j-1})/(\alpha\Delta y^2) = 0$$

or: $(\Phi_{xx} + \Phi_{yy})^n - \Delta t/\Delta x^2(2/\alpha - 1)\Phi_t - (\Delta t/\Delta x)\,\Phi_{xt} + (2\Delta t/\alpha)\Phi_{yyt} = 0$

or: $$\beta\Phi_{xt} + \gamma\Phi_{yyt} + \varepsilon\Phi_t = Re \qquad (3.4)$$

The importance of the transient term Φ_{xt} in an iterative method for transonic solutions can be demonstrated as follows.

The solution of compressible flows are normally determined from a system of the form:

$$[\,L\,]\,[\delta\Phi] = -R(\Phi) \qquad (3.5)$$

where [L] is chosen, for practical purposes, to be the incompressible Laplacian operator. This method will not converge for high transonic cases since the Laplacian cannot replace a mixed type operator. For mild transonic cases, the solution may converge if the artificial viscosity is greatly enhanced. However, convergence difficulties will re-appear if the grid is refined.

It is therefore more appropriate to design an iterative scheme that is based on the unsteady problem so that the converged solution is obtained when the steady state is reached.

For example, let us consider the one-dimensional unsteady equation in terms of the velocity potential:

$$\gamma\Phi_{tt} + 2u\,\beta\Phi_{xt} = (a^2 - u^2)\Phi_{xx} \qquad (3.6)$$

When the flow is supersonic, equation (3.6) is hyperbolic. It has been proven [5] that in order to have two real characteristics for the hyperbolic equation, one must have:

$$\beta^2 > 1 - 1/M^2 \qquad (3.7)$$

In other words, for the iterative scheme to succeed in supersonic regions, the coefficient of the Φ_{xt} term must be positive and

larger than $\sqrt{1-1/M^2}$.

The iterative matrix must be augmented by a Φ_{xt} term and should be modified by a term proportional to:

$$\Delta x \frac{\partial \Phi_t}{\partial x} = \Delta x \Delta t \frac{\partial}{\partial x}(\delta\Phi) \qquad (3.8)$$

$$= (\Phi_i - \Phi_{i-1})^{n+1}$$

The first term is added to the diagonal and the second to the RHS since the value of Φ on the line upstream is known.

The VLSOR scheme marching with the flow contains the Φ_{xt} term while other iterative methods such as point SOR, point Jacobi, horizontal line successive over-relaxation (HLSOR), line Jacobi, Fast Solver, VLSOR marching against the flow etc. do not have a Φ_{xt} term and must be explicitly added.

3.1.2 Zebroid Scheme

Instead of sweeping the field with vertical lines, a horizontal line solver can be applied. However, HLSOR produces a Φ_{yt} term of varying sign when applied to each line. If every second horizontal line is updated (Zebroid scheme), the transient term Φ_{yt} does not appear. An iterative step therefore requires two field sweeps. With a Φ_{xt} or Ψ_{xt} term explicitly added, the Zebroid method converges much faster than the VLSOR method [9]. This can be attributed to the fact that flow information is transmitted faster in the stream-wise direction in this method than in VLSOR.

3.2 Poisson Method

The nonlinear equation can be re-arranged in the following form:

$$(\Phi_{xx} + \Phi_{yy})^{n+1} = -(\rho_x \Phi_x + \rho_y \Phi_y)^n/\rho^n \qquad (3.9)$$

which suggests an iterative scheme of the form:

$$\{\rho_i\} \cdot [L]\{\delta\Phi\}^{n+1} = -\alpha \{Re\}^n \qquad (3.10)$$

where $[L]$ = incompressible operator or the Laplacian,

$= \nabla^2 = \partial_{xx} + \partial_{yy}$

$\delta\Phi^{n+1} = \Phi^{n+1} - \Phi^n$

$\{Re\}^n$ = residual at iteration level n

$= [K]^n \{\Phi\}^n - \{f\}^n$

α = acceleration factor $(1 \le \alpha \le 2)$

This method converges rapidly if $[L]$ is a good approximation of the actual compressible operator. An iteration scheme with the Prandtl-Glauert scale factor can also be applied to accelerate the convergence:

$$\rho_\infty [(1 - M_\infty^2)\, \partial_{xx} + \partial_{yy}]\{\delta\Phi\} = -\alpha \{Re(\Phi^n)\} \qquad (3.11)$$

3.3 Taylor Method

This method resembles the Poisson method above, except that the global stiffness matrix is assembled every iteration with the new density value.

$$(\rho^n \delta\Phi_x)_x + (\rho^n \delta\Phi_y)_y = -\alpha \{Re\}^n \qquad (3.12)$$

More work is required at each step due to the assembly but the total computation effort may be less.

It should be noted that neither Poisson nor Taylor method will converge for moderate to high transonic cases unless greatly enhanced artificial viscosity is used to stabilize the solution. Such solutions are "contaminated" and convergence problems will resurface if the grids are refined.

3.4 First- and Second-Degree Implicit Methods

It can be seen from the Poisson or Taylor method that a simulation of the type given by (3.10) or (3.12) can be employed and this idea is extended to an implicit scheme to involve the solutions at two or three consecutive iteration levels in the following manner:

$$\varepsilon [L] \{\delta^2\Phi\} + \alpha [L] \{\delta\Phi\} = -\beta \{Re\} \qquad (3.13)$$

where: [L] = Laplacian operator

ε = 0 for first degree method

= 1 for second degree method

α,β = acceleration parameters

The Φ_{xt} or Ψ_{xt} is needed and can be introduced by the following method. In elements with supersonic nodes, an asymmetric matrix can be constructed as:

$$[A] = [L]\,[T]$$

where $[T_{ij}]$ is a transformation to exclude the influence at a supersonic point from downstream nodes while doubling that from nodes upstream. This can be schematically seen in Fig 3.1. The global matrix is then decomposed by an LU scheme. The iteration is more laborious at each step but global convergence is found to be certain for transonic solutions.

Another method to introduce the Φ_{xt} for this scheme is to modify the Laplacian matrix as:

$$[\,L\,]\{\delta\Phi\} + [\,L_1]\{\delta\Phi\} = -\{Re\} \qquad (3.14)$$

where $[\,L_1\,]$ is an asymmetric operator whose elements are:

$$L_1 = (1 - 1/M^2)\{\Phi_i - \Phi_{i-1}\} \qquad (3.15)$$

In our work, the solution is started from a guess, which can logically be chosen to be the incompressible one. Either the Poisson or the Taylor method can suitably be applied for some preset number of cycles or until convergence difficulty is encountered (this is normally when the

supersonic region appears). The iteration scheme is then switched to either the first- or second-degree implicit method, with transient terms Φ_{xt} and Ψ_{xt} explicitly introduced as described above, until the global convergence is met.

CHAPTER 4
NUMERICAL RESULTS

The numerical results of transonic flows in a one-dimensional nozzle and of a two-dimensional flow around an isolated non-lifting NACA0012 airfoil will be presented in this chapter with details.

4.1 One-Dimensional Flow

With the introduction of the modified potential, a non-isentropic solution may be obtained following the algorithm shown in Flowchart 4.1.

Starting with an intial guessed value of potential at the exit Φ_{ex}, (or equivalently $\Delta\Phi$ across the nozzle), the solution is found subject to a certain convergence criterion, say when the maximum residue of either the potential equation (2.4) or the pressure equation (2.7) is below 10^{-6}. The pressure determined at the exit is compared against the required value and a new value of Φ_{ex} is computed using an interpolation or extrapolation scheme, such as the secant method. The outer loop is restarted until the calculated and the prescribed back pressures agree within a tolerance of 10^{-3}.

The computational grid with 50 linear elements for the velocity potential equation and 51 elements for the pressure equation is shown superimposed in Fig. 4.2. The numerical solution is illustrated in Fig. 4.3 against the exact solution for a static back pressure of 12.41 psia and $\Delta\Phi$ = 0.651.

It can be seen that the theoretical and numerical solutions are in satisfactory accordance.

The convergence histories of solutions with different features are shown in Fig. 4.4.

For the potential equation, the Poisson iteration method is carried out for a preset number of iteration steps or until at least one supersonic node appears. The first-degree implicit method, augmented by a Φ_{xt} term, is then applied until convergence is met. The Poisson method is employed throughout the iteration process for the pressure equation.

In addition, the important role of the transient term Φ_{xt} in the convergence of transonic solutions is clearly demonstrated in Fig. 4.4 for the above case. The influence of the artificial viscosity on the shock location and strength, as discussed in Chapter 2, is also illustrated in Fig. 4.5.

4.2 Two-Dimensional Flow

The computational algorithm in this case is presented in Flowchart 4.6.

Several options exist in the program that can be specified to obtain one of the followings:

(1) classical potential solution

(2) non-isentropic potential solution with entropy correction given by Rankine-Hugoniot relation

(3) modified potential solution with perturbation stream function.

At every iteration step, the global stiffness matrix is assembled using the so-called "Skyline" method [22] which makes use of the sparse

character of the matrix to economize computer storage. In this method, the bandwidth of each row is stored along with the addresses of the diagonal elements. The assembled matrix contains only non-zero elements. The system is then decomposed and inverted by the LU decomposition scheme.

It is worth also describing the method to determine the nodal values of velocity and vorticity of an element. The velocity and vorticity at the Gaussian points are first obtained from the potential and perturbation stream function solutions. These values are then extrapolated to the corner nodes using the procedure described in Ref. [23]. This scheme is found quite accurate and particularly important for vorticity.

In transonic test cases, the Taylor iteration method is used for the first few iterations until one supersonic node appears. The first-degree implicit method is then applied with the term Φ_{xt} or Ψ_{xt} explicitly added in the same manner as described in Chapter 3. A relaxation factor of unity is used throughout the iteration process.

Note that since the vorticity equation is only secondary, it need not be solved at every iteration step. Here, it is solved periodically, i.e. every 5 iterations.

The computational grid, shown in Fig. 4.7, consists of 51 nodes on the airfoil surface and 28 nodes from the airfoil surface to the outer boundaries, which is located at 3.5 chord lengths from the blade surface. Some extremely fine layers adjacent to the airfoil are found to be crucially necessary to represent the large vorticity variation in that region.

The Mach number distribution over the airfoil surface for a subsonic flow ($M_\infty = 0.72$) is shown in Fig. 4.8 against the classical potential solution. No difference should be expected since the flow is isentropic and no vorticity is generated.

Transonic results with far field Mach numbers 0.80 and 0.85 are illustrated in the next series of figures. The classical full potential solution and the new potential-perturbation stream function are plotted against each other. The trends of an Euler solver are observed, namely that the shock weakens and moves upstream. These solutions cannot , however, be directly compared to those, for example, in Ref. [24], considering the much finer grid used in the latter, which could hardly be afforded on the Concordia Cyber 825.

The Mach number contours, the perturbation stream function contours and the vorticity contours for the two solutions can be found in Figs. 4.11-12.

The non-dimensional vorticity as a function of the lateral direction is plotted for various stations are shown in Figs. 4.13-14. Note that the vorticity on the solid boundary is zero since the shock wave is normal to the airfoil surface and also vanishes along the wake due to symmetry.

The convergence histories for the two test cases are shown in Figs. 4.15-16.

4.3 Discussion

It is now clear that modifications of the classical potential model are feasible to obtain non-isentropic rotational solutions without actually having to solve the full Euler equations.

Two non-isentropic models have been presented in this Thesis and have been applied to the flow in a nozzle and for a two-dimensional external flow. Both models yield unique solutions.

Two methods of calculating the entropy have also been

proposed: the first via a correction provided by the Rankine-Hugoniot relations across the shock and the second by solving a second-order pressure equation to yield the stagnation loss across the shock. The finite element method was shown to simplify the solution with the natural boundary conditions for the pressure equation easily accounted for.

In the two-dimensional case, the rotational effects are introduced through the addition of a correction term in the form of a perturbation stream function. The vorticity equation does not have the singularity problem as the full stream function formulation. Among the advantages of this method over the primitive variables formulation are the fewer number of equations to be solved and the much simpler boundary conditions for both Φ and Ψ'.

References

[1] Murman, E.M. and J.D. Cole, "Calculations of Plane Steady Transonic Flows," AIAA Journal, Vol. 9, pp. 114-121, 1971.

[2] Garabedian, P.R. and D.G. Korn, "Analysis of Transonic Airfoils," Communications of Pure and Applied Mathematics, Vol. 24, pp. 841-851, 1971.

[3] Jameson, A., "Iterative Solution of Transonic Flows Over Airfoils and Wings, Including Flows at Mach 1," Communications of Pure and Applied Mathematics, Vol. 27, pp. 283-309, 1974.

[4] Hafez, M.M., J.C. South and E.M. Murman, "Artificial Compressibility Methods for Numerical Solutions of Transonic Full Potential Equation," AIAA Journal, Vol. 17, pp. 838-844, 1978.

[5] Habashi, W.G., "Potential Flows," Finite Element Method in Fluid Mechanics and Heat Transfer Course Notes, Concordia University - Pratt and Whitney Canada - Purdue University, 1983.

[6] Habashi, W.G., E.G. Dueck and D.P. Kenny, "Finite Element Approach to Compressor Blade-to-Blade Cascade Analysis," AIAA Journal, Vol. 17, pp. 693-698, 1979.

[7] Deconinck, H. and Ch. Hirsch, "Finite Element Methods for

Transonic Blade-to-Blade Calculation in Turbomachines," ASME Journal of Engineering for Power, Vol. 103, pp. 665-667, 1981.

[8] Habashi, W.G. and P.L. Kotiuga, "Numerical Solution of Subsonic and Transonic Cascade Flows," International Journal for Numerical Methods in Fluids, Vol. 2, pp. 317-330, 1982.

[9] Habashi, W.G. and M.M. Hafez, "Finite Element Solutions of Transonic Flow Problems," AIAA Journal, Vol. 20, No. 10, pp. 1368-1376, 1982.

[10] Steinhoff, J. and A. Jameson, "Multiple Solutions of the Transonic Potential Flow Equation," AIAA Journal, Vol. 20, No.11, pp. 1521-1525,1982.

[11] Salas, M.D., A. Jameson and R.E. Melnik, "A Comparative Study of the Nonuniqueness Problem of the Potential Equation," Proceedings of the 6th AIAA Computational Fluid Dynamics Conference, Danvers, Mass., pp. 48-60, 1983.

[12] Hafez, M.M. and D. Lovell, "Entropy and Vorticity Corrections for Transonic Flows," Proceedings of the 6th AIAA Computational Fluid Dynamics, Danvers, Mass., pp. 630-644, 1983.

[13] Habashi, W.G., M.M. Hafez, and P.L.Kotiuga, "Computation of Choked and Supersonic Turbomachinery Flows by a Modified Potential Method," AIAA Journal, Vol. 23, No. 2, pp. 214-220, 1985.

[14] Habashi, W.G. and M.M. Hafez, "Finite Element Stream Function Solutions of Transonic Rotational Internal and External Flows," Journal of Numerical Methods for Partial Differential Equations, Vol. 1, No. 2, pp. 127-144, 1985.

[15] Hafez, M.M. and D. Lovell, "Numerical Solution of Transonic Stream Function Equation," AIAA Journal, Vol. 21, No. 3, pp. 327-335, 1983.

[16] Hirsch, Ch. and H. Deconinck, "A Survey of Finite Element Methods for Transonic Flows," **Numerical Methods in Aeronautical Fluid Dynamics** (Ed. P.L. Roe), Academic Press, London, 1982, pp. 143-188.

[17] Yee, H.C., R.M. Beam and R.F. Warming, "Stable Boundary Approximations for a Class of Implicit Schemes for the One-Dimensional Inviscid Equations of Gas Dynamics," AIAA Paper 81-1009, 1981.

[18] Deconinck, H. and Ch. Hirsch, "Boundary Conditions for the Potential Equation in Transonic Internal Flow Calculations," ASME Paper 83-GT-135, 1983.

[19] Hafez, M., W.G. Habashi and P.L. Kotiuga, "Conservative Calculations of Non-Isentfopic Transonic Flows," International Journal for Numerical Methods in Fluids, Vol. 5, No. 12, pp. 1047-1057, 1985.

[20] Peeters, M.F., W.G. Habashi and E. Dueck, "Finite Element Solutions of the Navier-Stokes Equations," in print, International Journal for Numerical Methods in Fluids, 1985.

[21] Carnahan, B., H.A. Luther and J.O. Wilkes, **Applied Numerical Methods**, John Wiley and Sons, New York, N.Y., 1969.

[22] Bathe, K.-J. and E.L. Wilson, **Numerical Methods in Finite Element Analysis**, Prentice-Hall, Englewood Cliffs, N.J., 1976.

[23] Hinton, E., F.C. Scott and R.E. Ricketts, "Local Least Squares Stress Smoothing for Parabolic Isoparametric Elements," International Journal for Numerical Methods in Engineering, Vol. 9, No. ,1975, pp. 235-239.

[24] Jameson, A., "Transonic Aerofoil Calculations Using the Euler Equations," **Numerical Methods in Aeronautical Fluid Dynamics**, (ed. P.L. Roe), Academic Press, London, 1982, pp.289-308.

APPENDIX
NONDIMENSIONALIZATION SCHEME

The solution should be best presented as non-dimensional variables with respect to the flow characteristic quantities for generality purpose. The non-dimensionalization scheme is summarized below with the normalized variables denoted by a superscript *.

(1) Length

$$x^* = x/c \; ; \; y^* = y/c$$

where c is the airfoil chord length.

(2) Velocity

$$u^* = u/a_o \; ; \; v^* = v/a_o$$

where a_o is the stagnation speed of sound. The local Mach number can be found by:

$$M^2 = M_o^2/[1 - (\gamma - 1)/2 \, M_o^2]$$

$$= (q/a_o)^2/[1 - (\gamma - 1)/2 \, (q/a_o)^2]$$

(3) Thermodynamic variables

$$p^* = p/p_o$$

$$T^* = T/T_o$$

$$\rho^* = \rho/\rho_o$$

where the subscript o denotes stagnation conditions.

(4) Potential and Perturbation Stream Function

To determine the non-dimensional potential Φ^* and perturbation stream function Ψ^*, we start with the definition of velocity:

$$u = \Phi_x + (1/\rho)\,\Psi'_y$$

which can be re-arranged as:

$$u^* a_o = (\partial\Phi/\partial x^*)/c + (1/\rho_o\rho^*)\,(\partial\Psi/\partial y^*)/c$$

or:

$$u = \partial\Phi/(ca_o\partial x^*) + (1/\rho_o\rho^*)\,\partial\Psi/(ca_o\partial y^*)$$

$$= \partial\Phi^*/\partial x^* + (1/\rho^*)\,\partial\Psi^*/\partial y^*$$

which implies:

$$\Phi^* = \Phi/(ca_o)$$

$$\Psi^* = \Psi/(c\rho_o a_o)$$

(5) Vorticity

From the definition of vorticity, one can write:

$$\omega = \partial v/\partial x - \partial u/\partial y$$

$$= (a_o/c)\,[\partial v^*/\partial x^* - \partial u^*/\partial y^*]$$

or: $$\omega = (a_o/c)\ \omega^*$$

The Crocco relation is now:

$$(a_o/c)\ \omega^* = (a/\gamma M)\ \partial(\Delta s/R)/(c\partial n^*)$$

or: $$\omega^* = (a/a_o)/\gamma M\ \partial(\Delta s/R)/\partial n^*$$

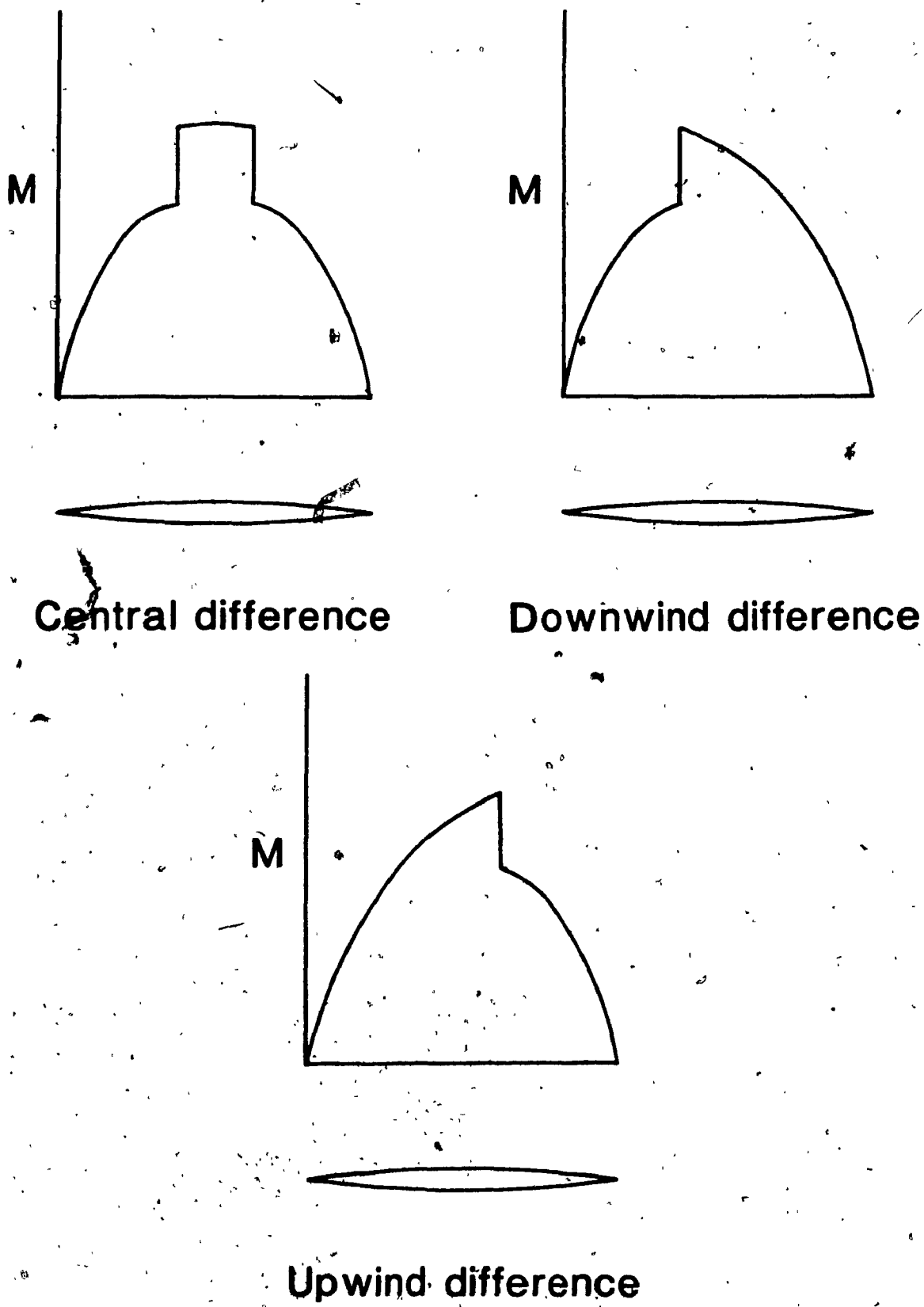

Fig. 1.1 Transonic Potential Solutions over a Biconvex Airfoil

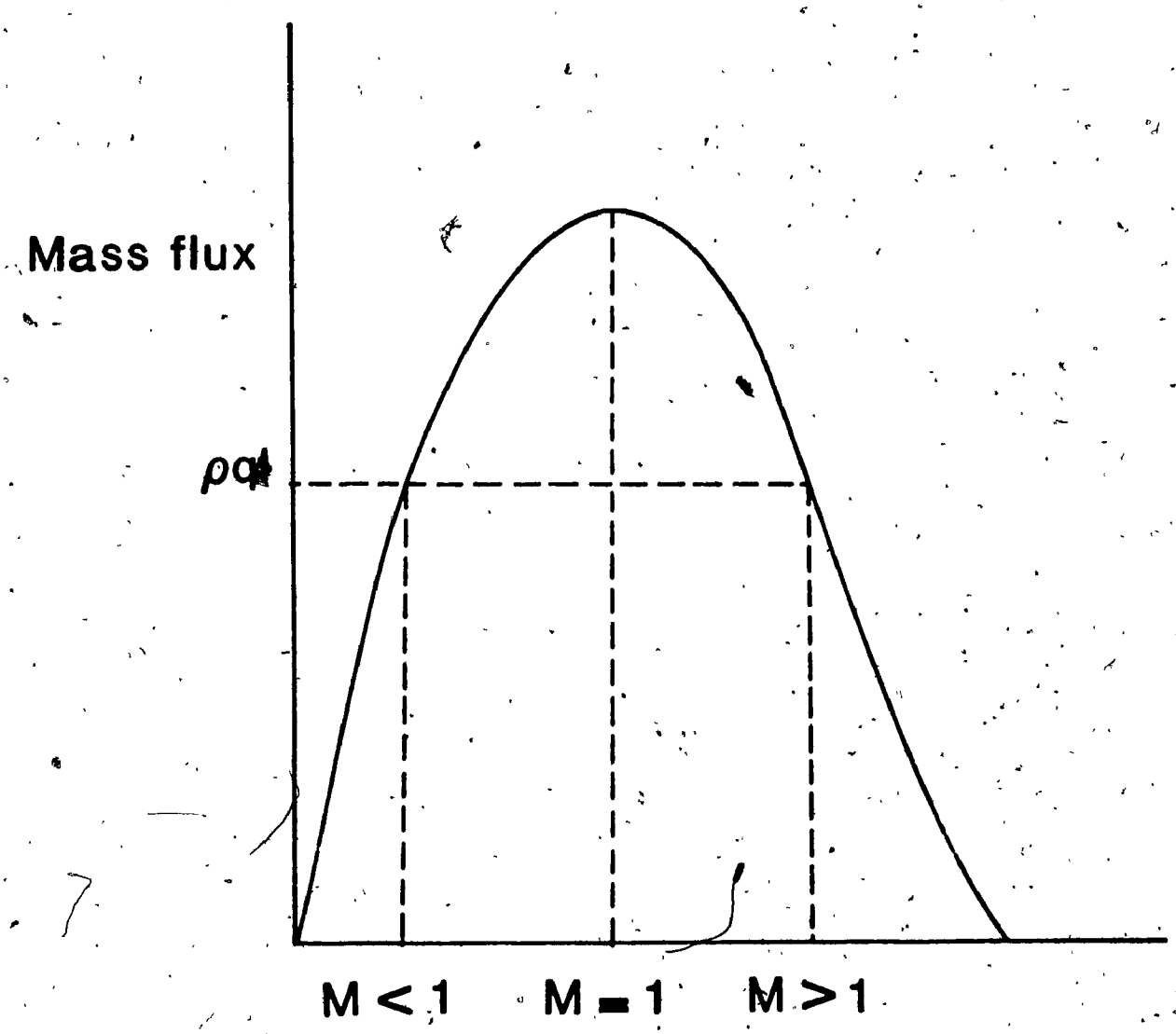

Fig 1.2 Mass flux vs. Mach number

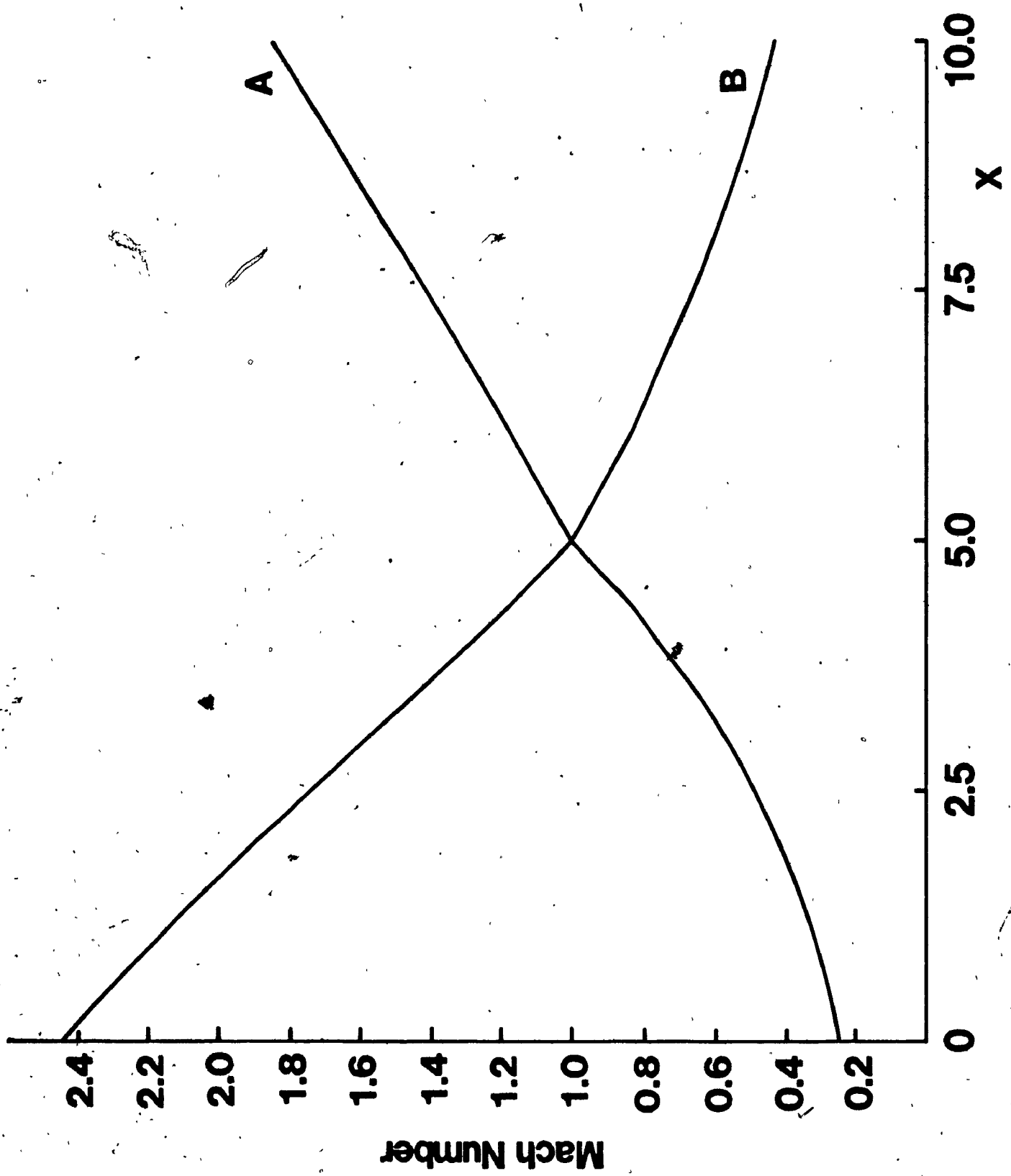

Fig. 2.1 Analytical Solution (Quasi One-dimensional Nozzle Flow)
(after Habashi, Hafez and Kotiuga [13])

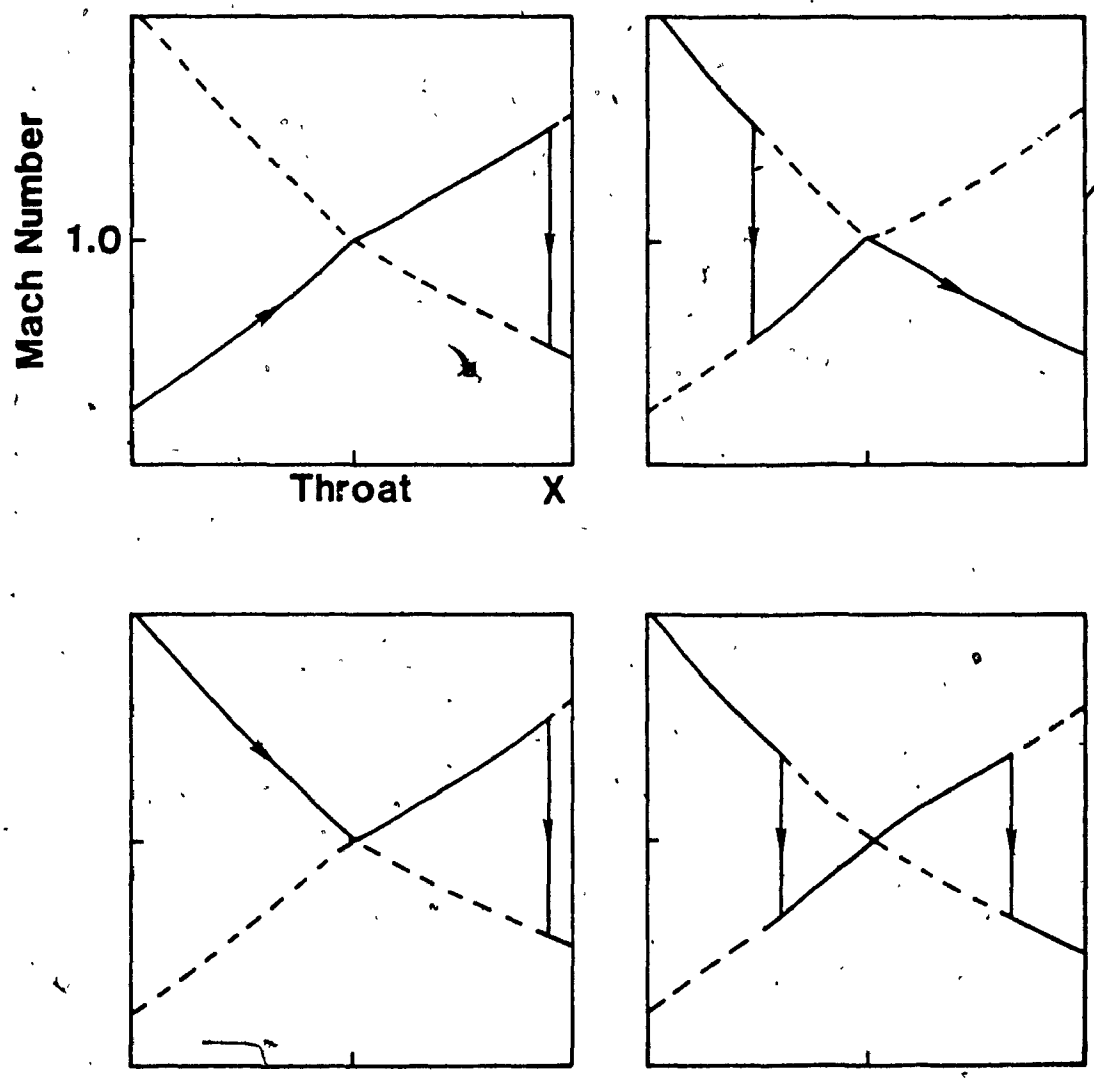

Fig. 2.1(cont.) Analytical Solution (Quasi One-dimensional Nozzle Flow)
(after Habashi, Hafez and Kotiuga [83])

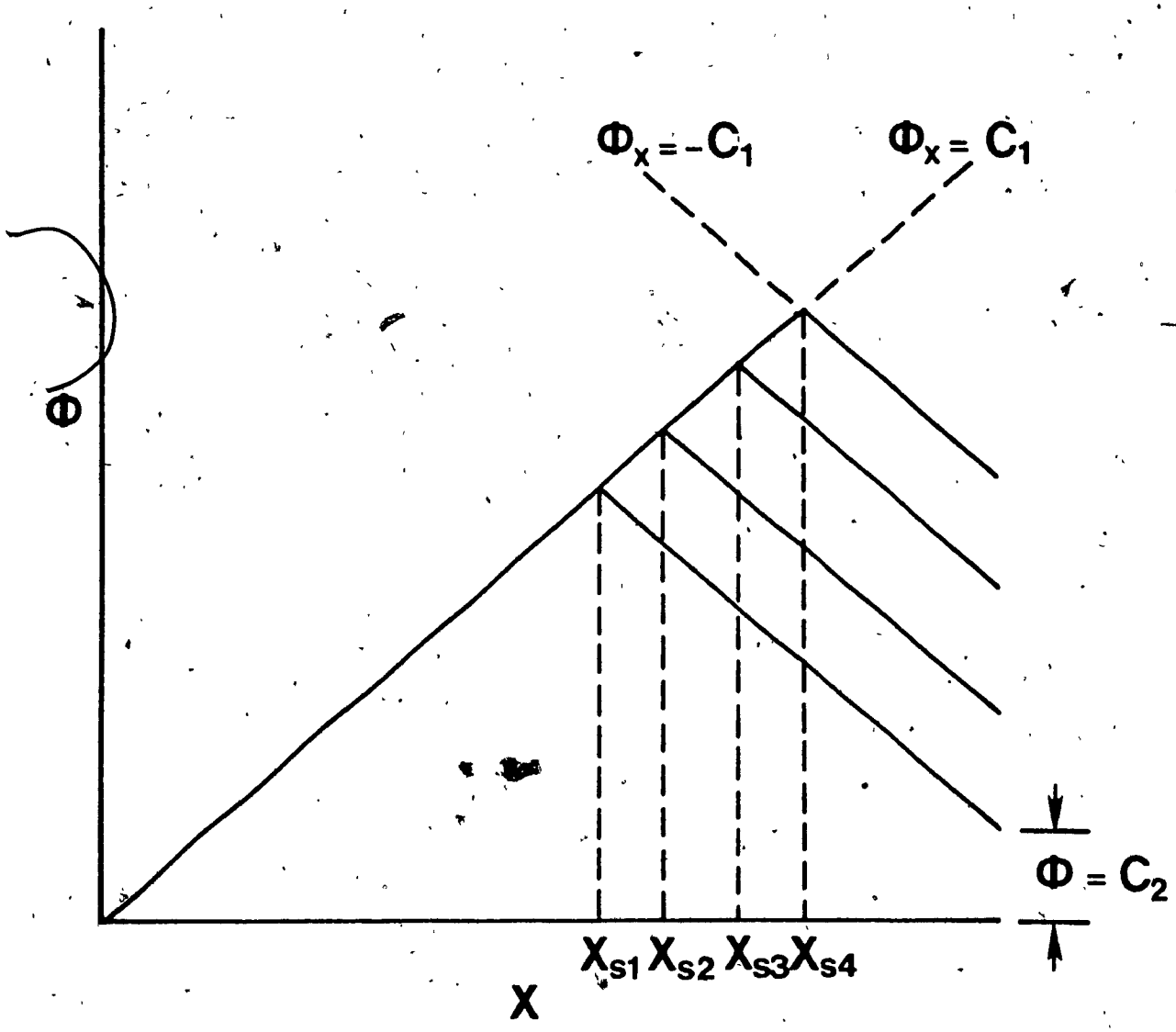

Model equation $[\Phi_x^2]_x = 0$

Fig. 2.2 Non-uniqueness of the Potential Solution

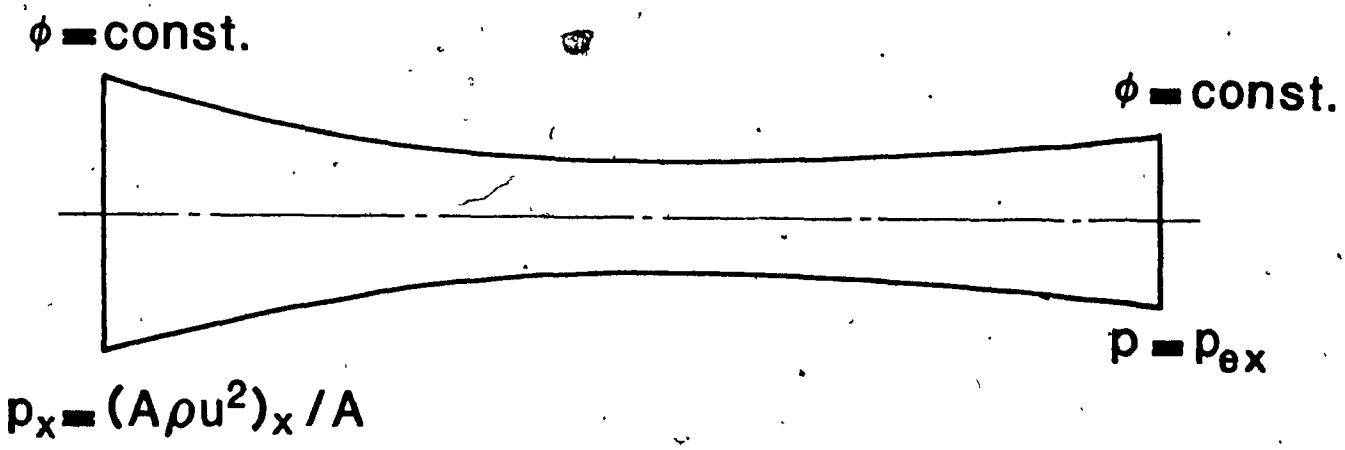

Fig. 2.2 Boundary Conditions for Quasi One-dimensional Flow

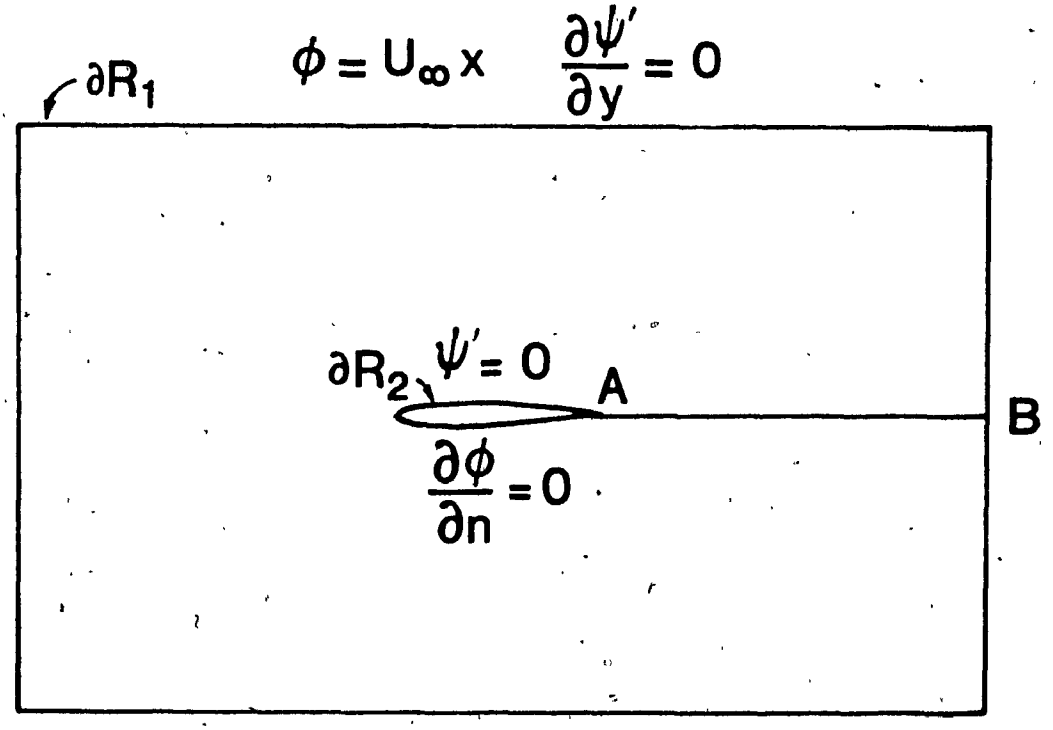

Fig. 2.3 Boundary Conditions for Two-dimensional Flow

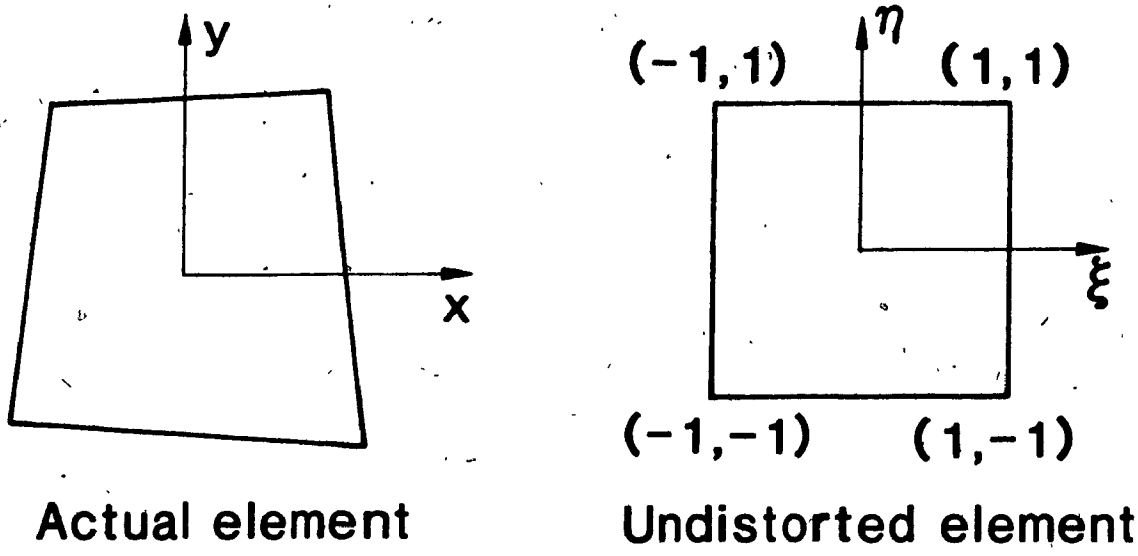

Fig. 2.4 Actual and Undistorted Elements

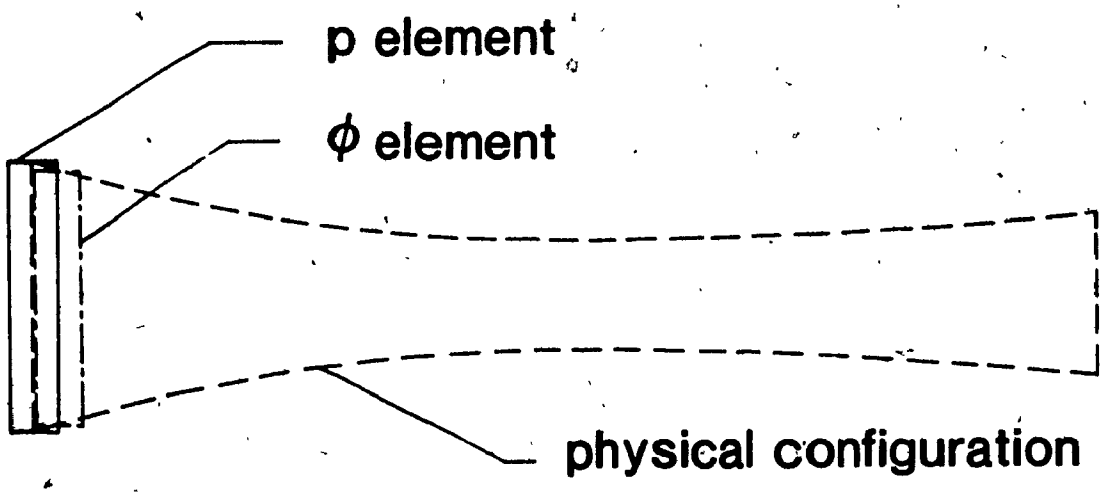

Fig. 2.5 Staggered Grid for Potential + Pressure Solution

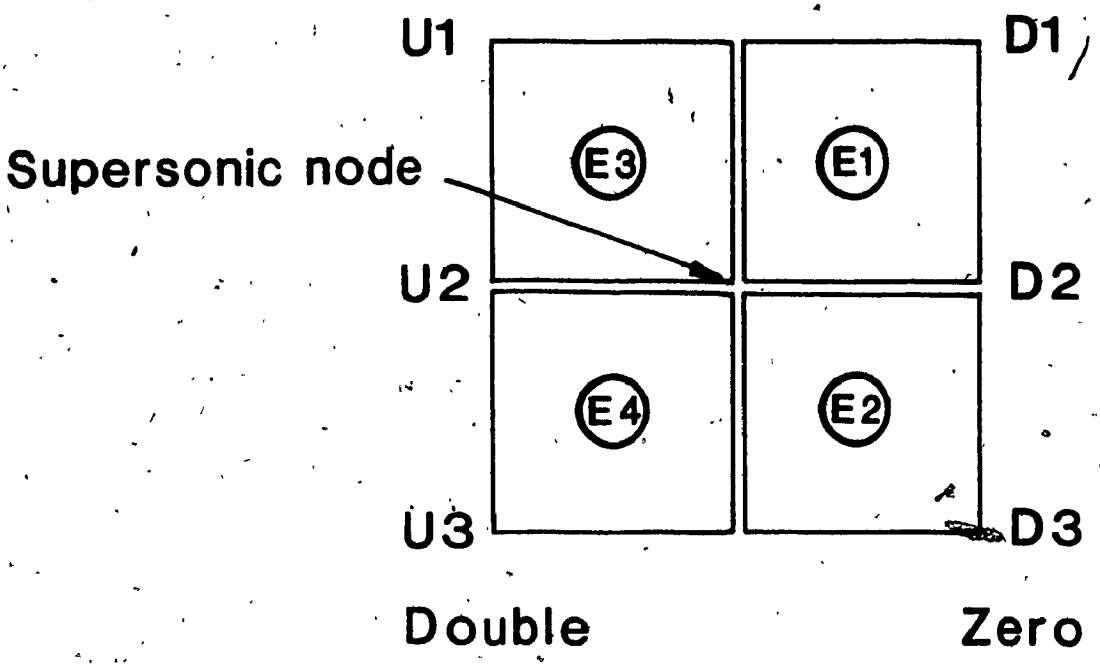

Fig. 3.1 Implementation of Φ_{xt} term

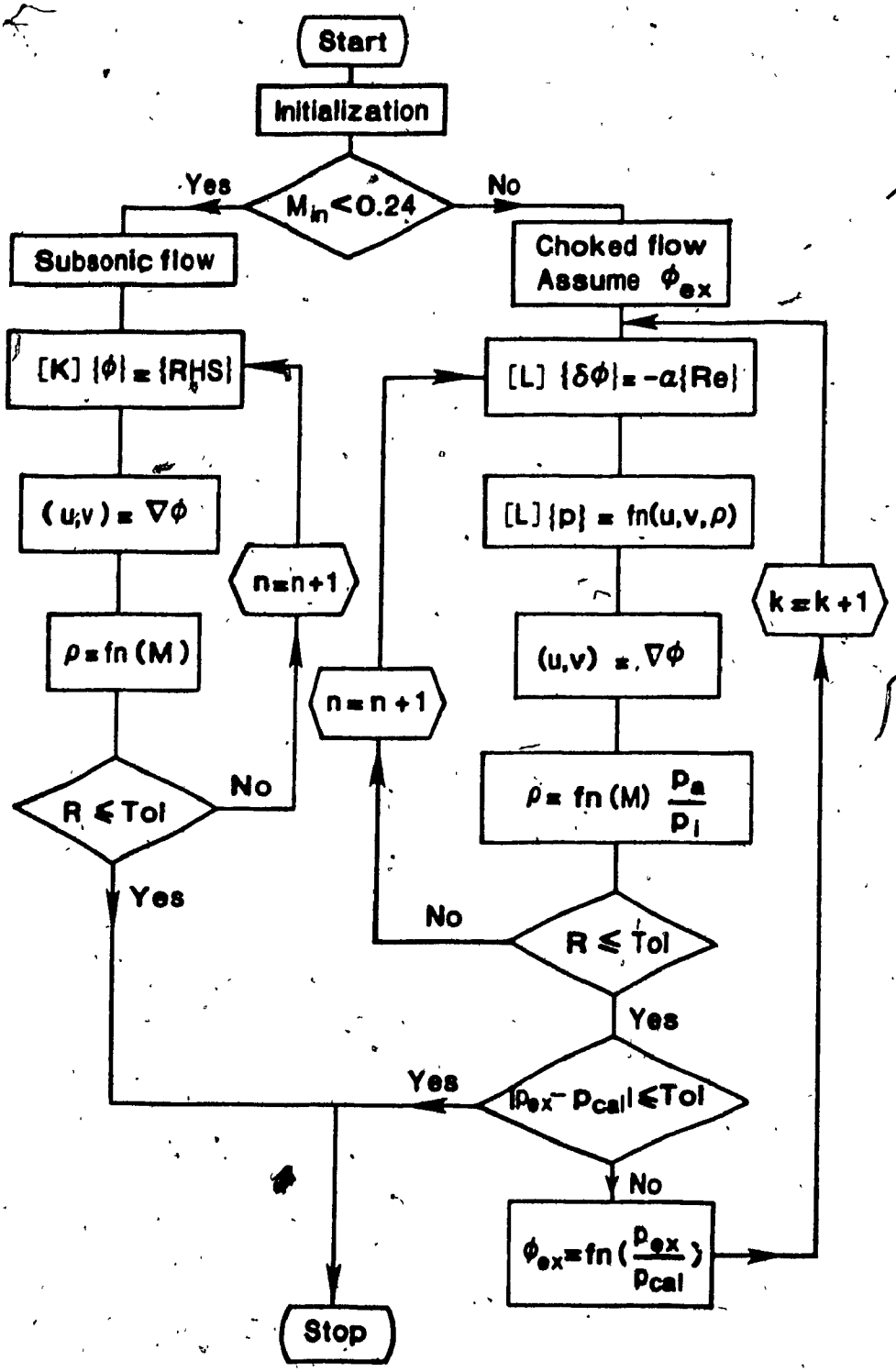

Fig. 4.1 Flowchart for One-dimensional Solution

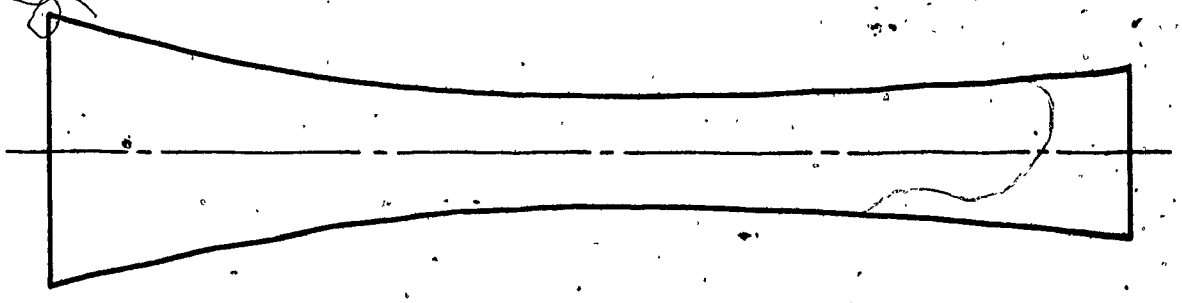

$$A(x) = 1 - 0.5(1 - 0.2x)^2 \quad 0 \leq x \leq 5$$

$$A(x) = 1 - 0.5(0.2x - 1)^2 \quad 5 \leq x \leq 10$$

Fig. 4.2 Computational Nozzle

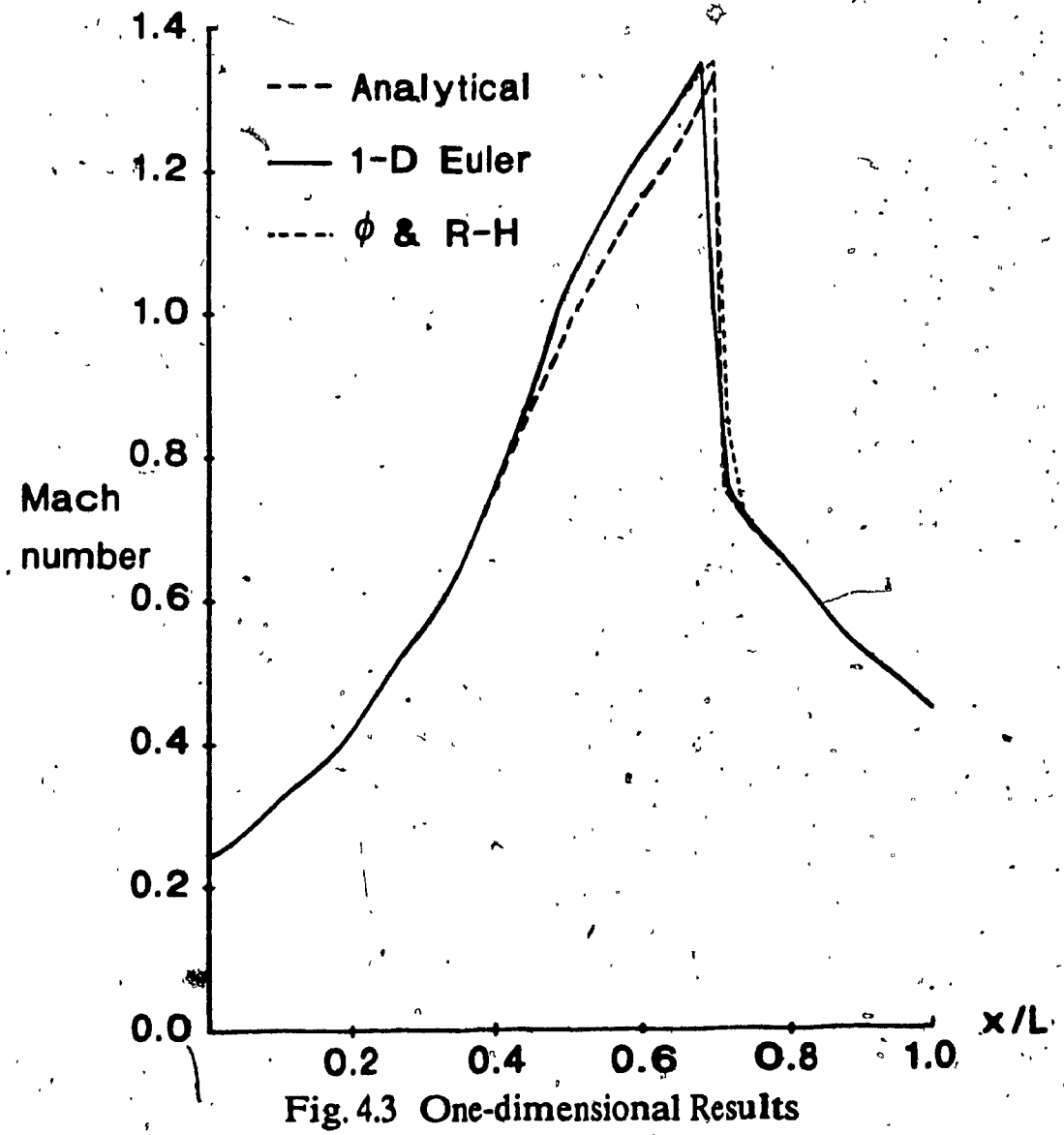

Fig. 4.3 One-dimensional Results

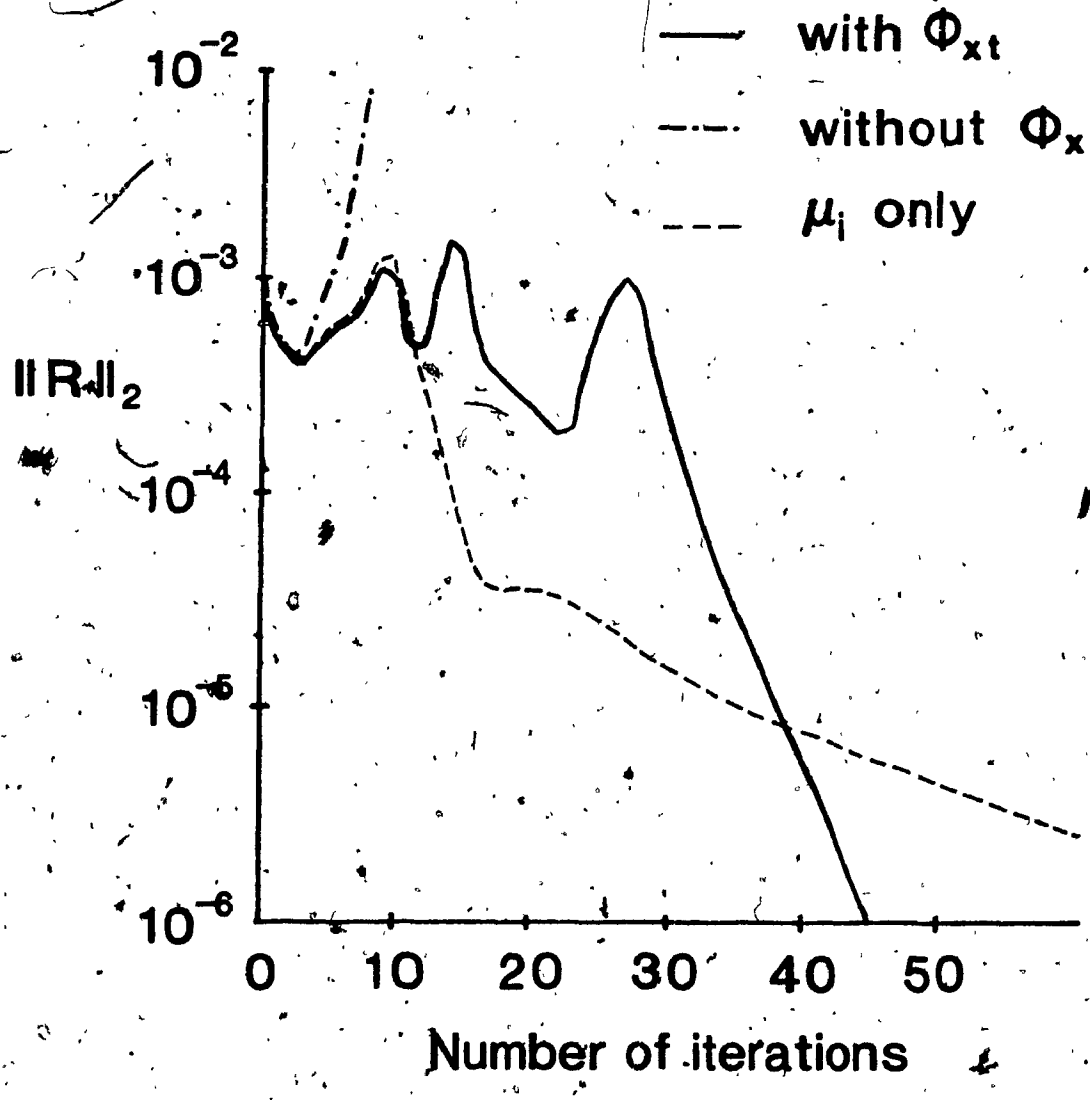

Fig. 4.4 Convergence History

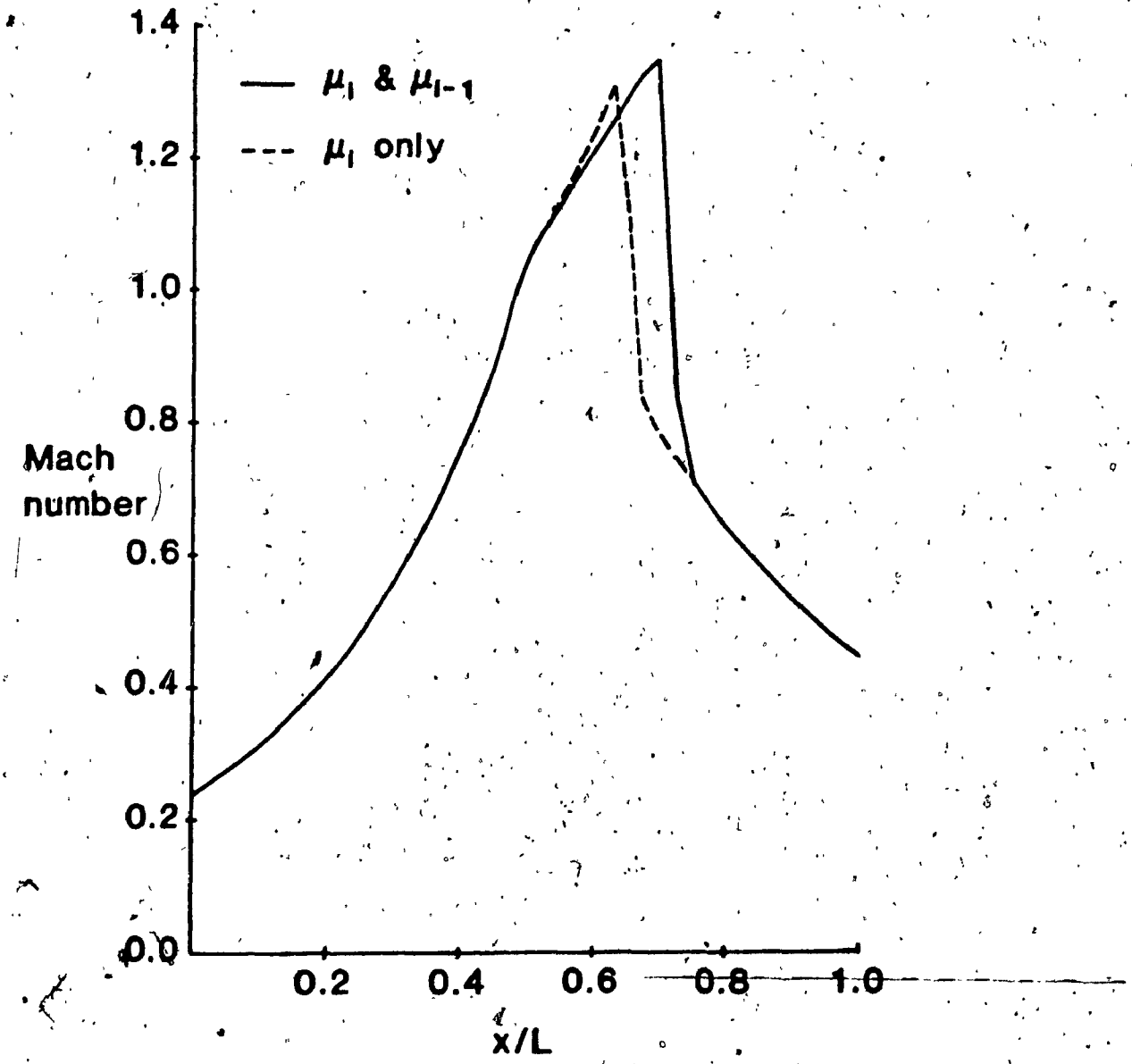

Fig. 4.5 Influence of Artificial Viscosity

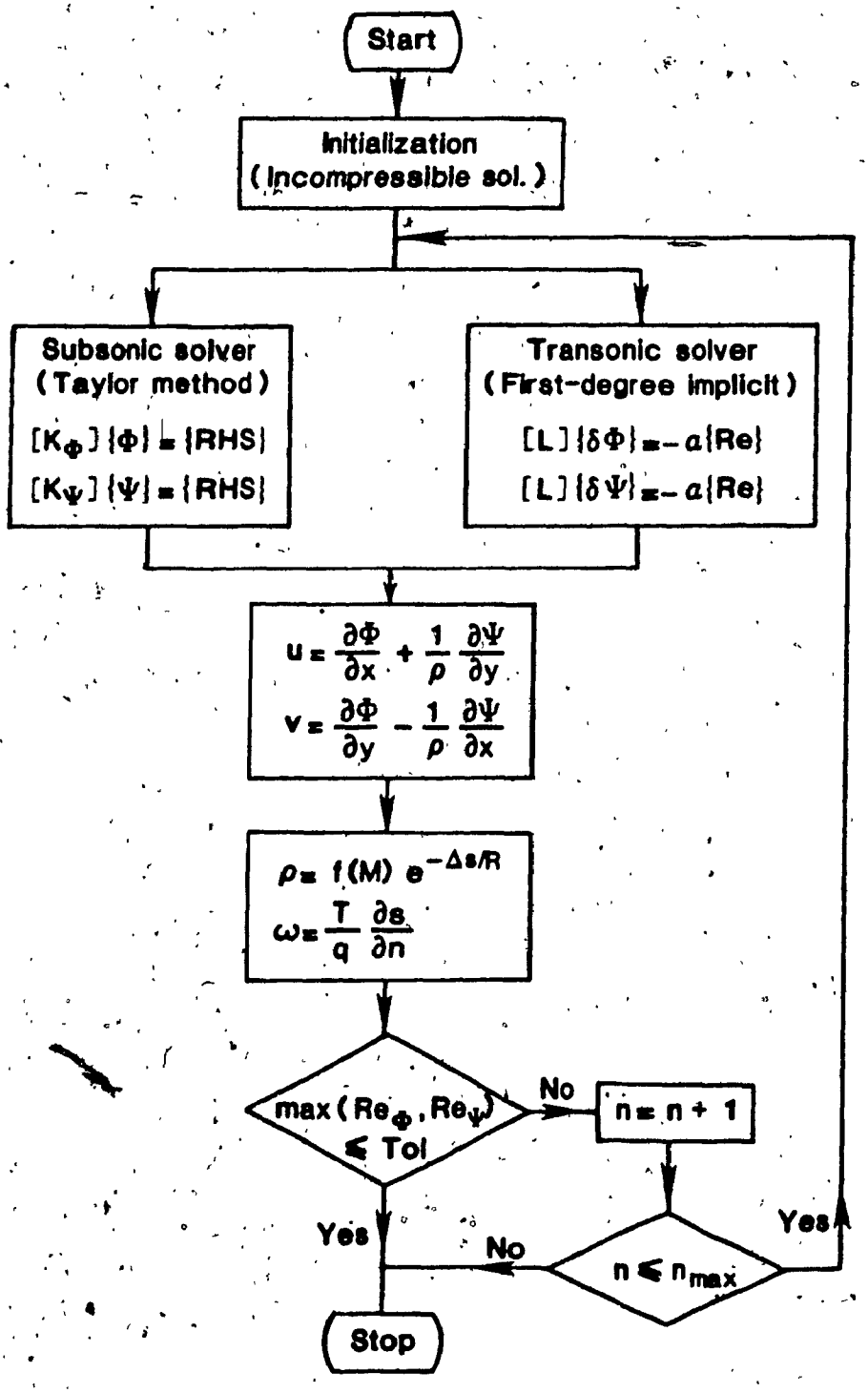

Fig. 4.6 Flowchart for Two-dimensional Solution

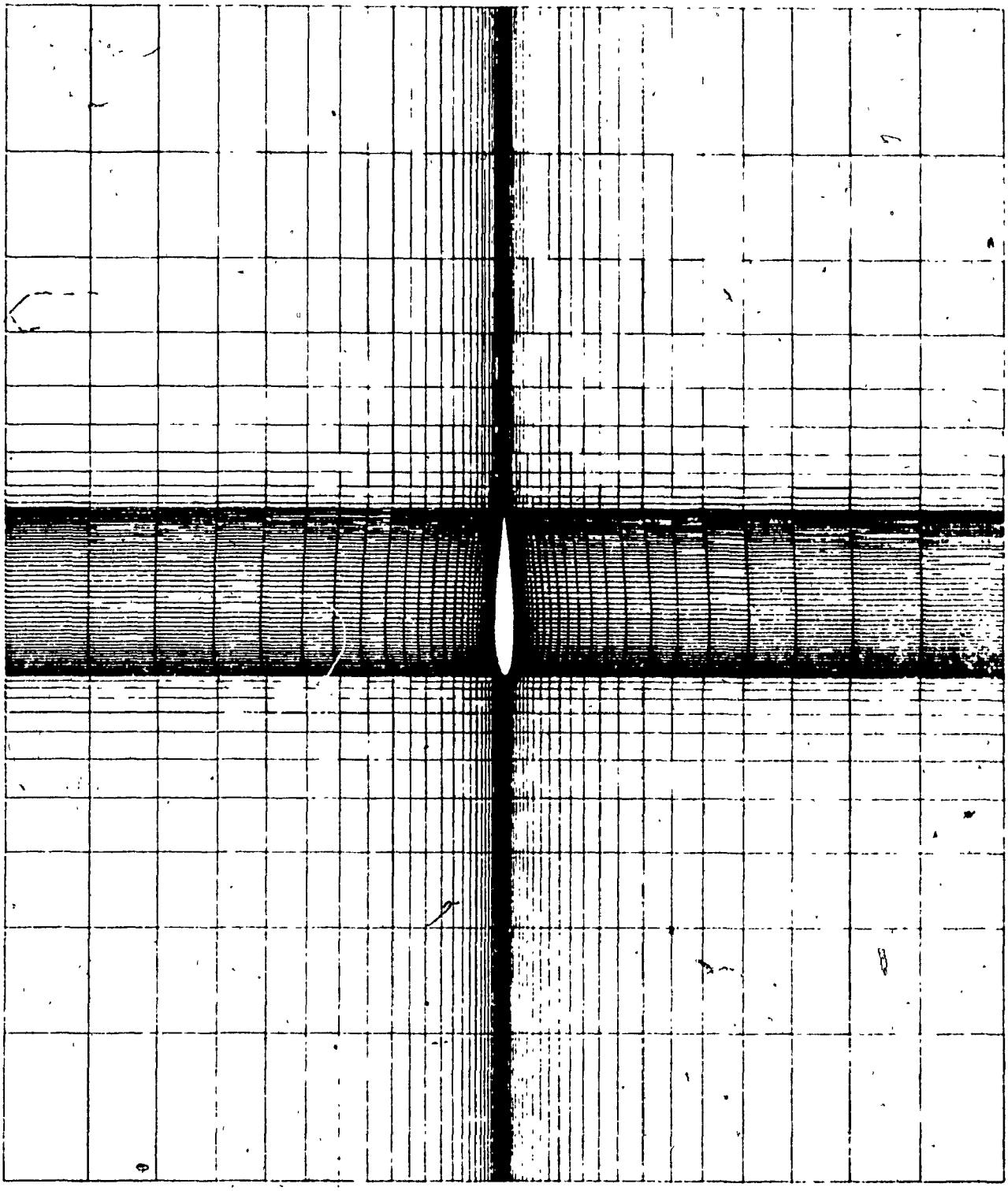

Fig. 4.7 Computational Grid for Airfoil

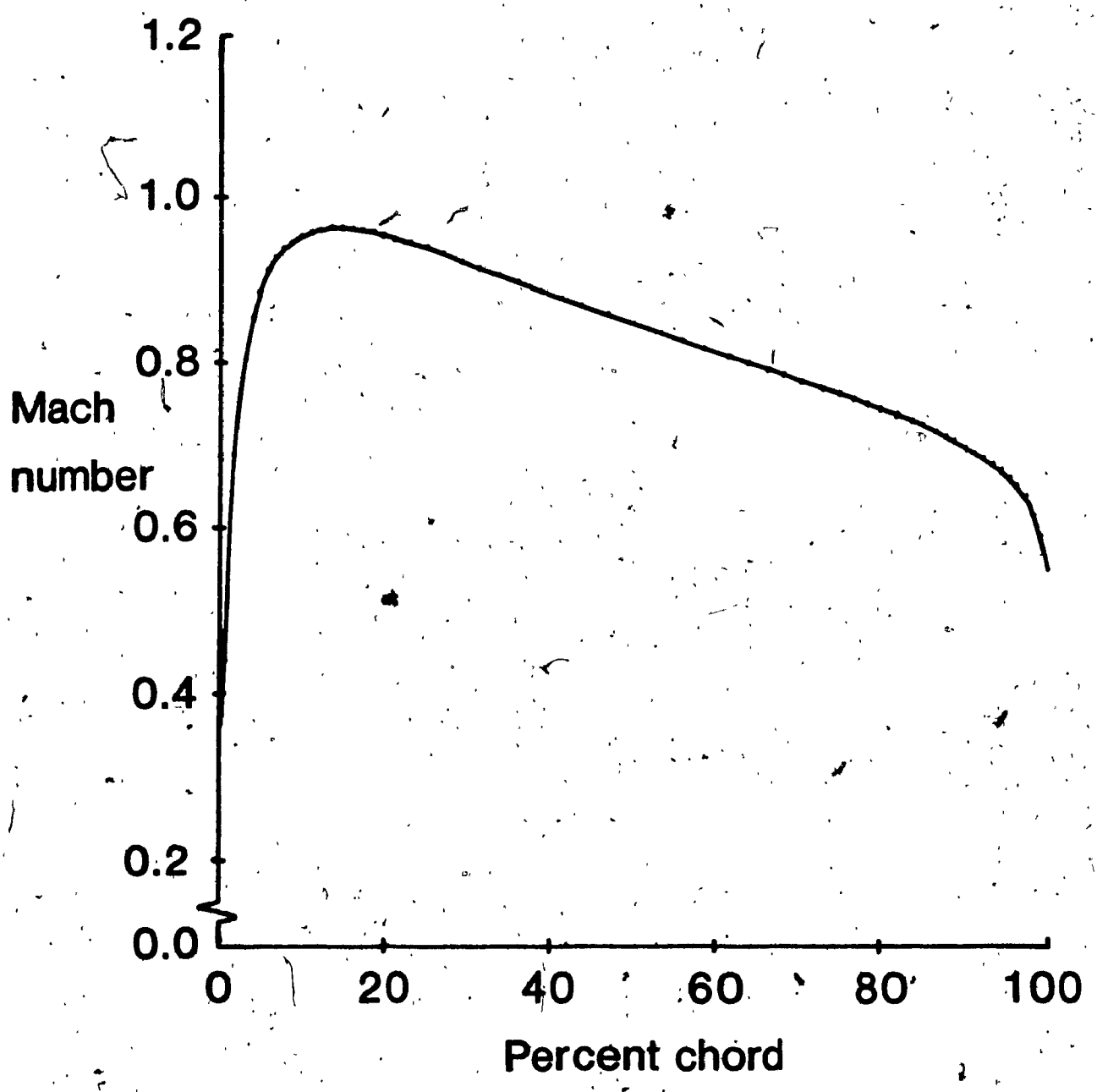

Fig. 4.8 Subsonic Solution

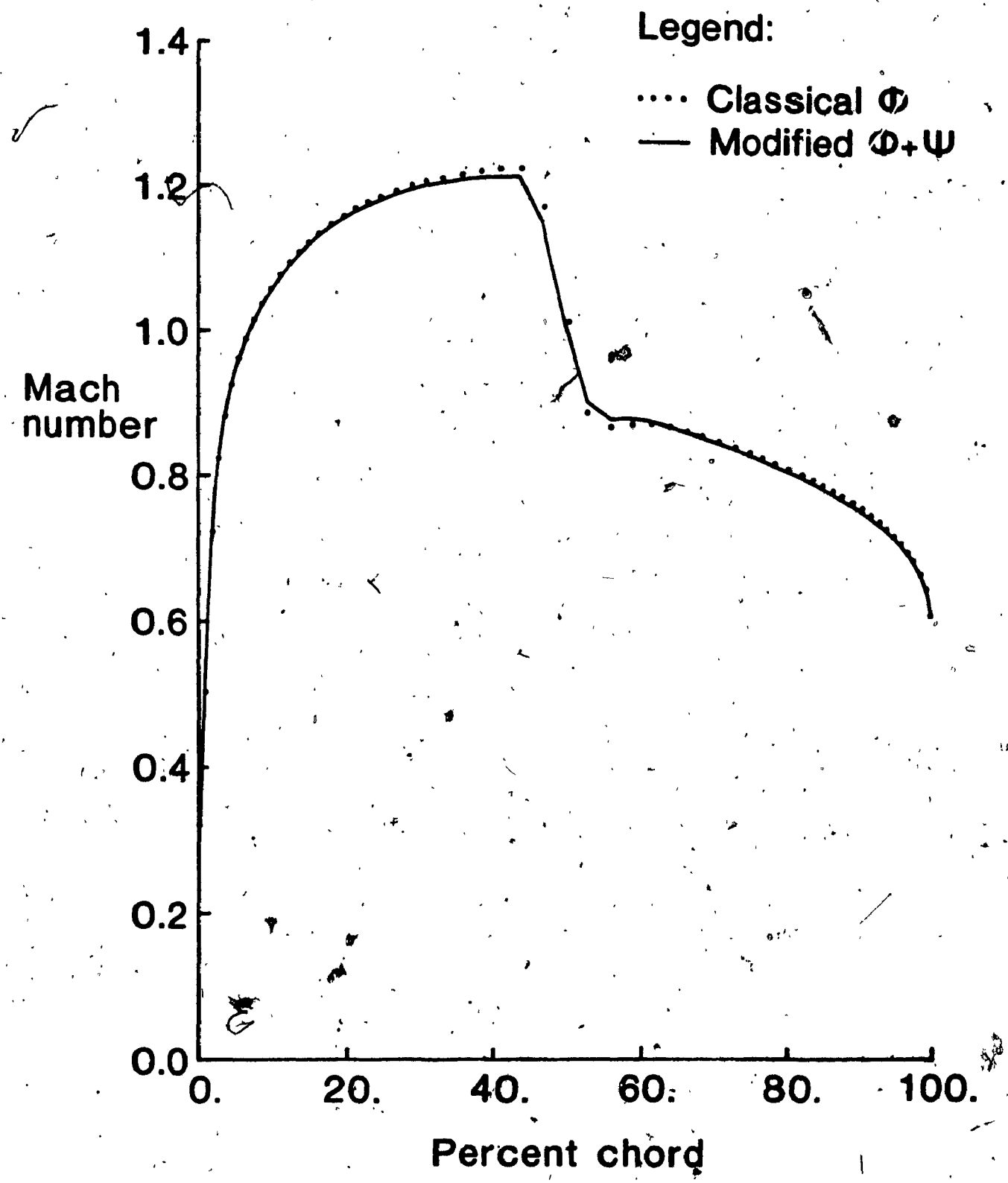

Fig. 4.9 Mach Number Distribution over Airfoil Surface (M_∞=0.80)

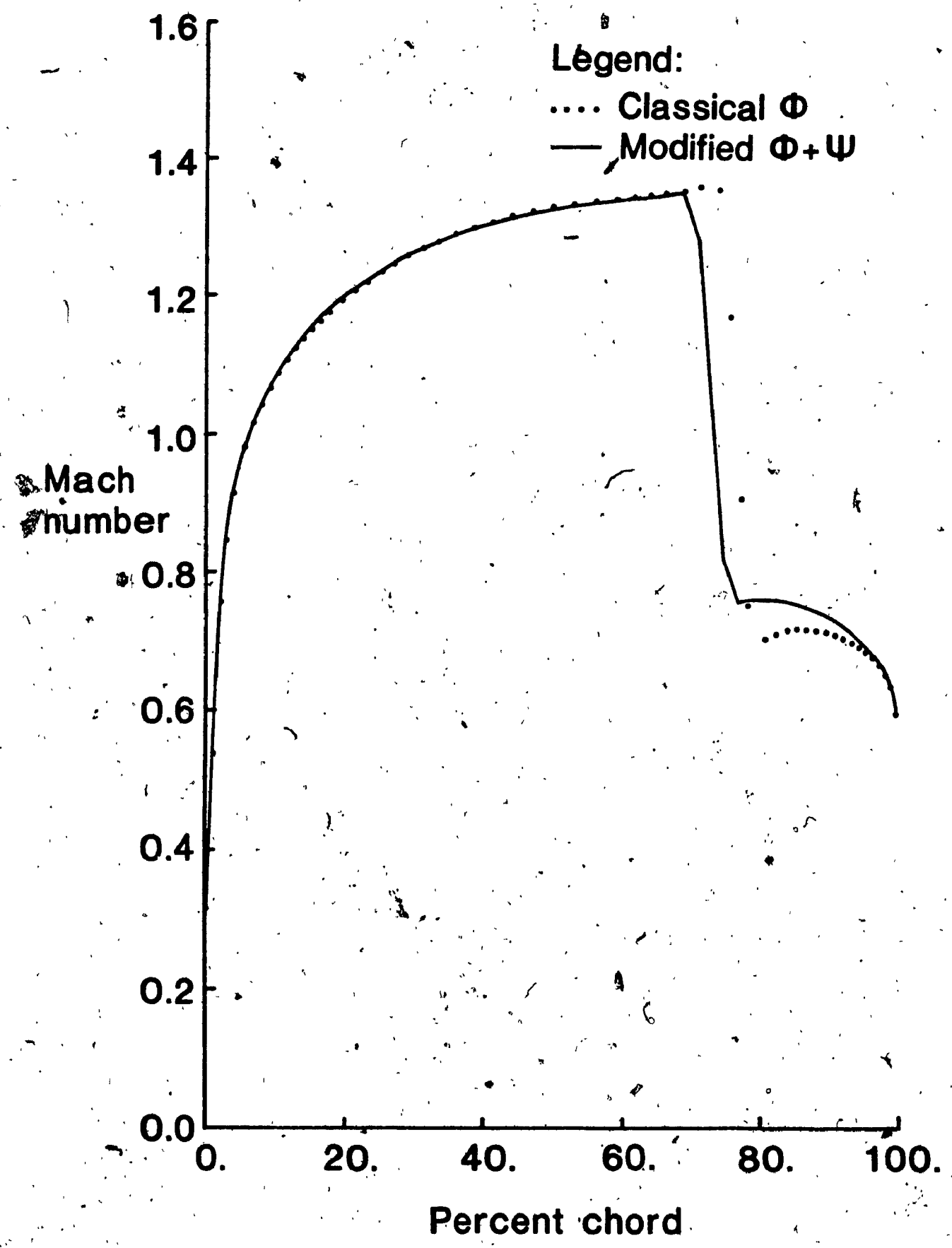

Fig. 4.10 Mach Number Distribution over Airfoil Surface (M_∞=0.85)

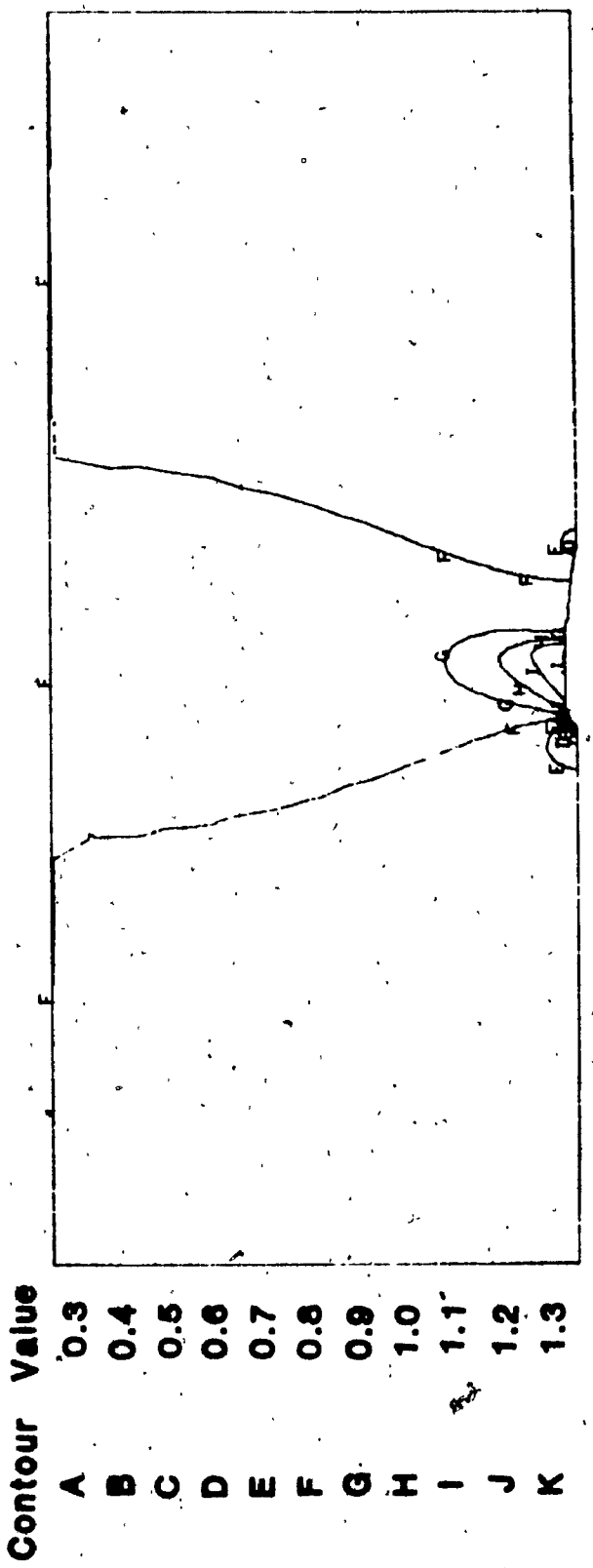

Fig. 4.11a Iso-Mach Contours (M_{∞}=0.80)

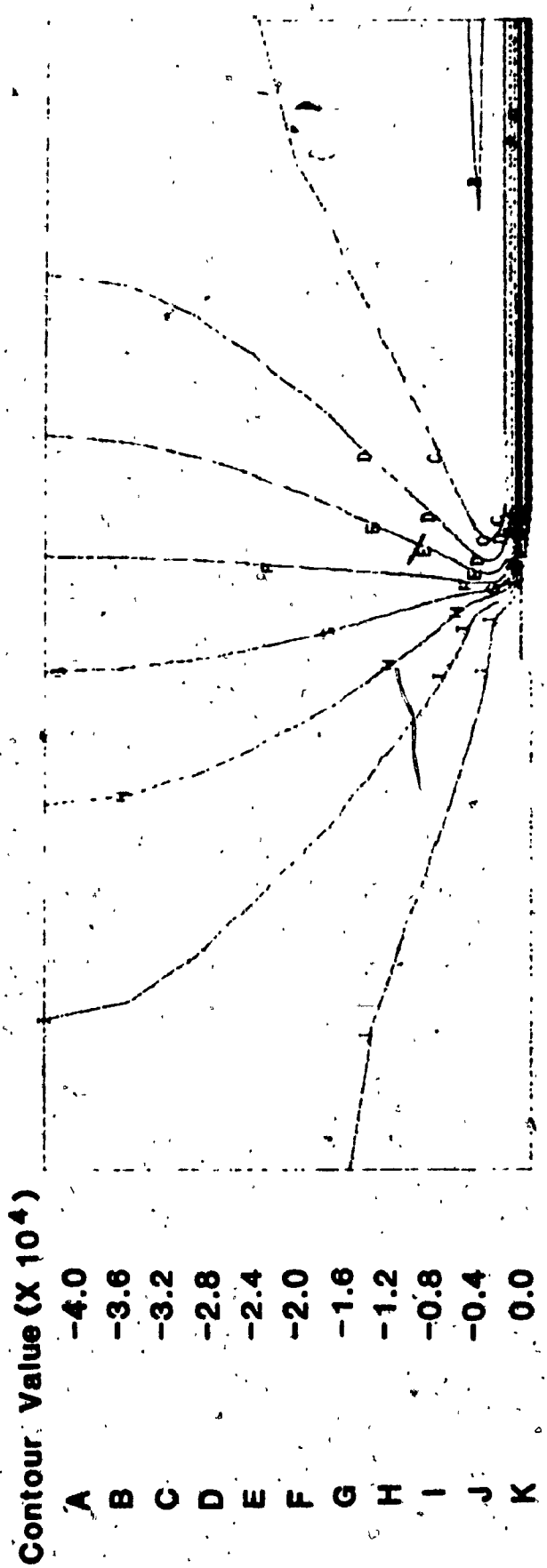

Fig. 4.11b Constant Stream Function Contours (M_∞=0.80)

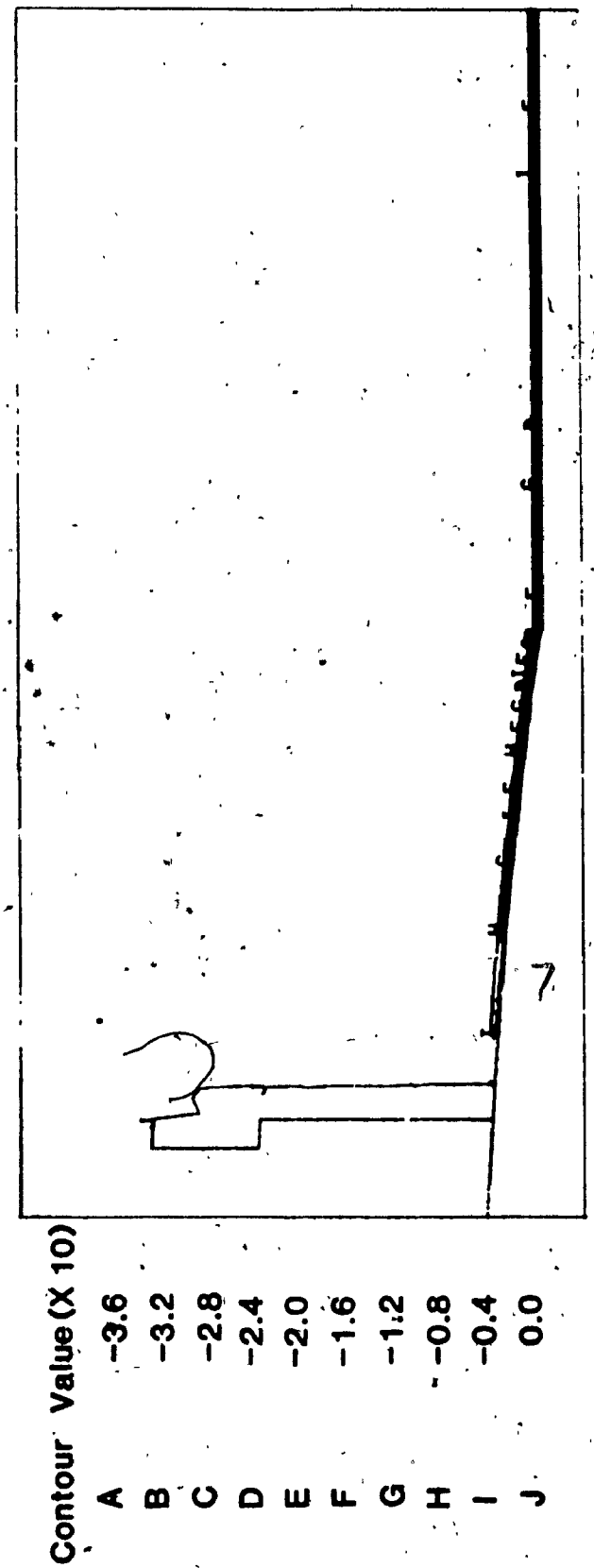

Fig. 4.11c Constant Vort[illegible]Contours (M_∞=0.80)

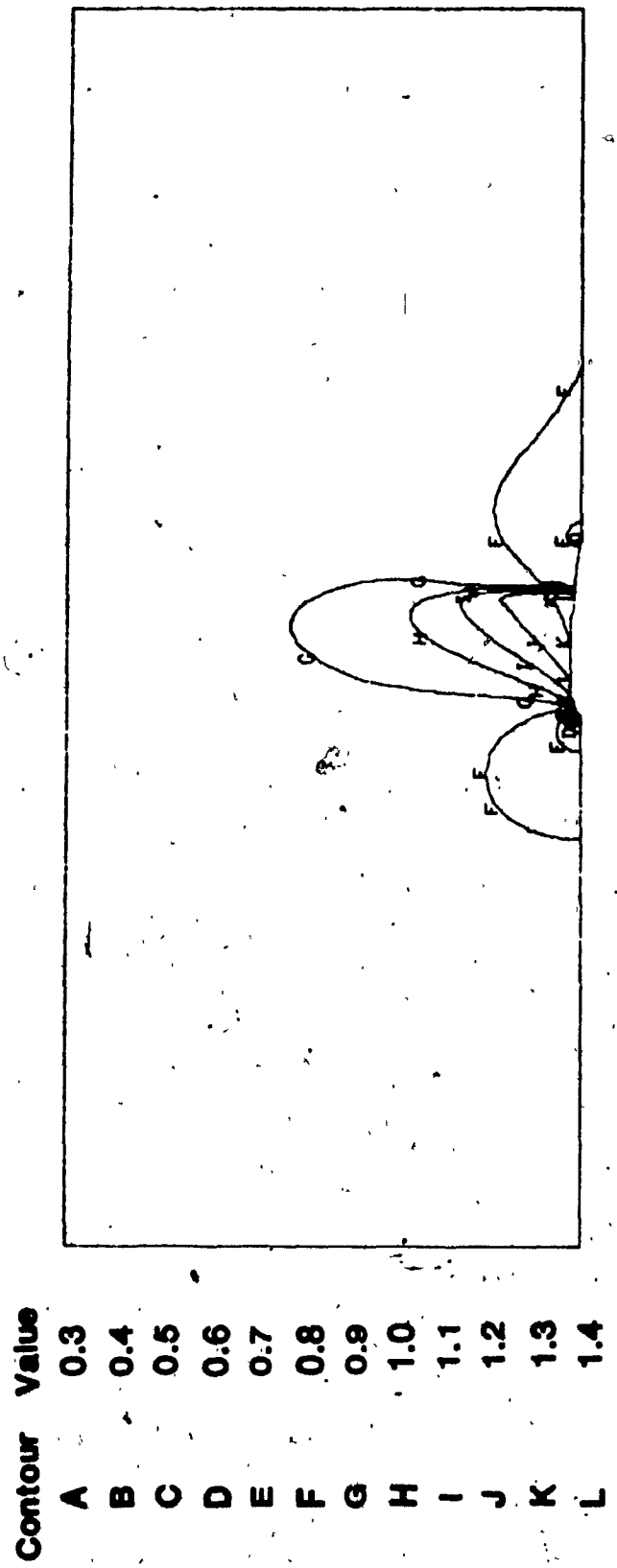

Fig. 4.12a Iso-Mach Contours (M_∞=0.85)

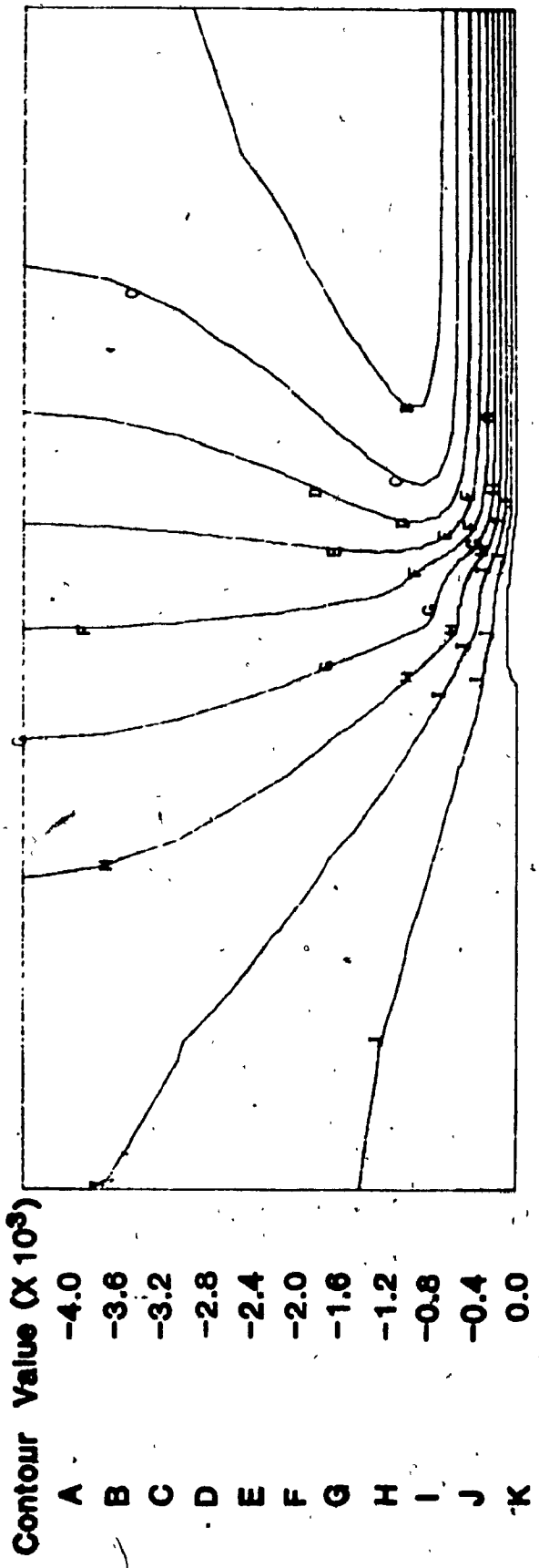

Fig. 4.12b Constant Stream Function Contours (M_∞=0.85)

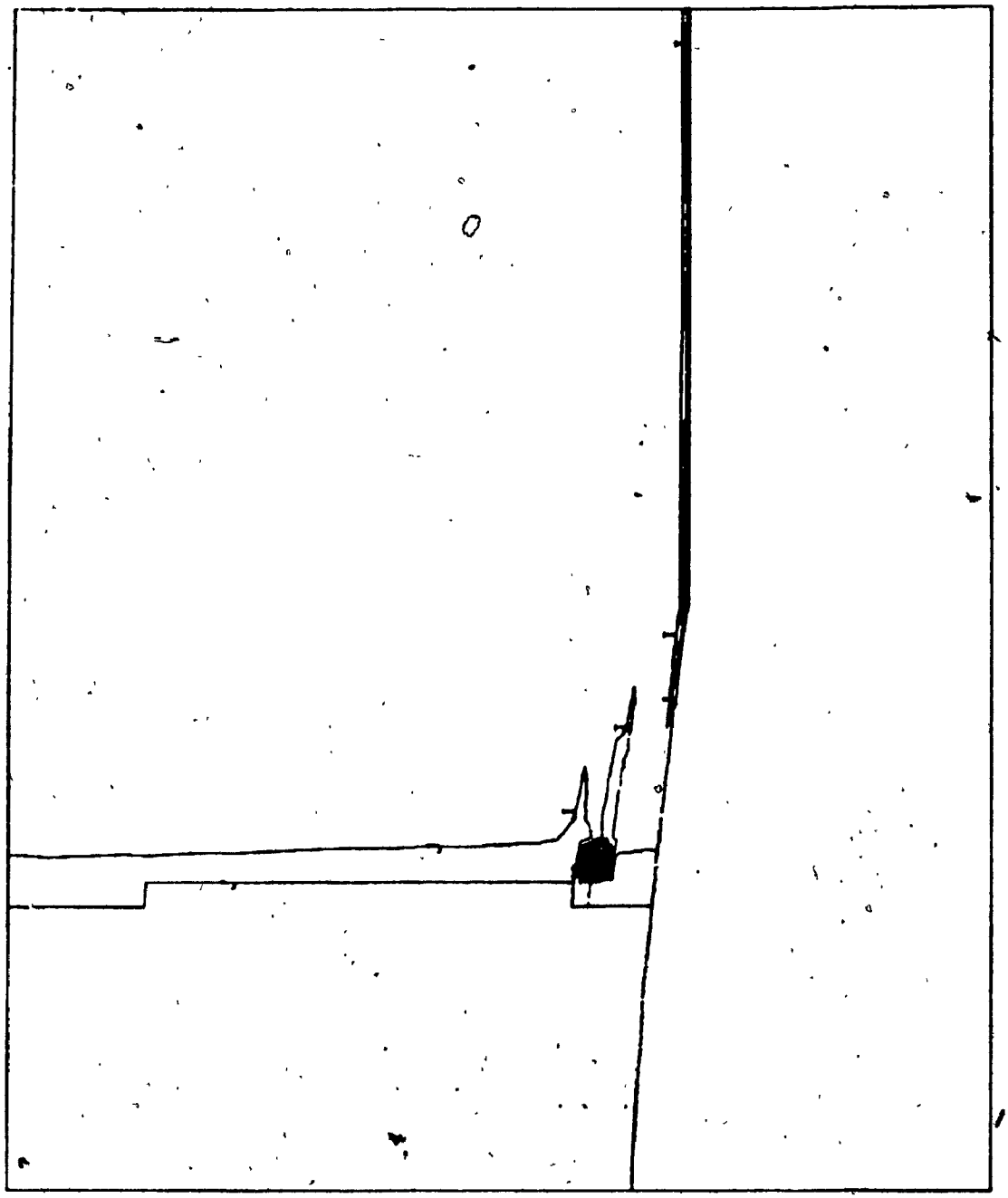

Fig. 4.12c Constant Vorticity Contours (M_∞=0.85)

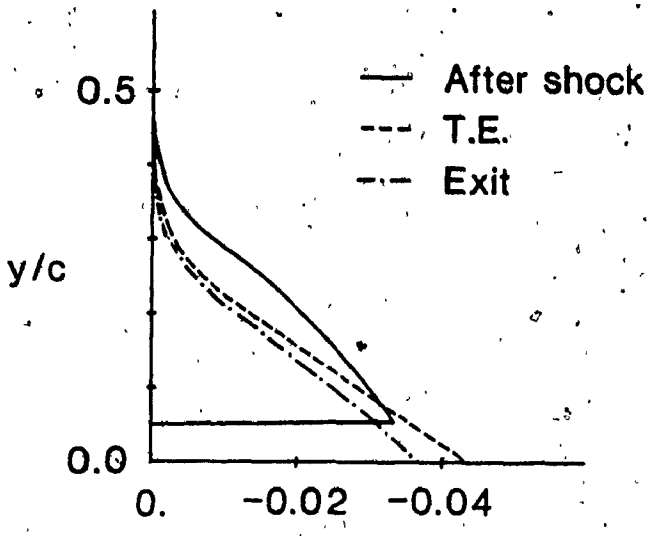

Fig. 4.13 Vorticity vs. Lateral Direction (M_∞=0.80)

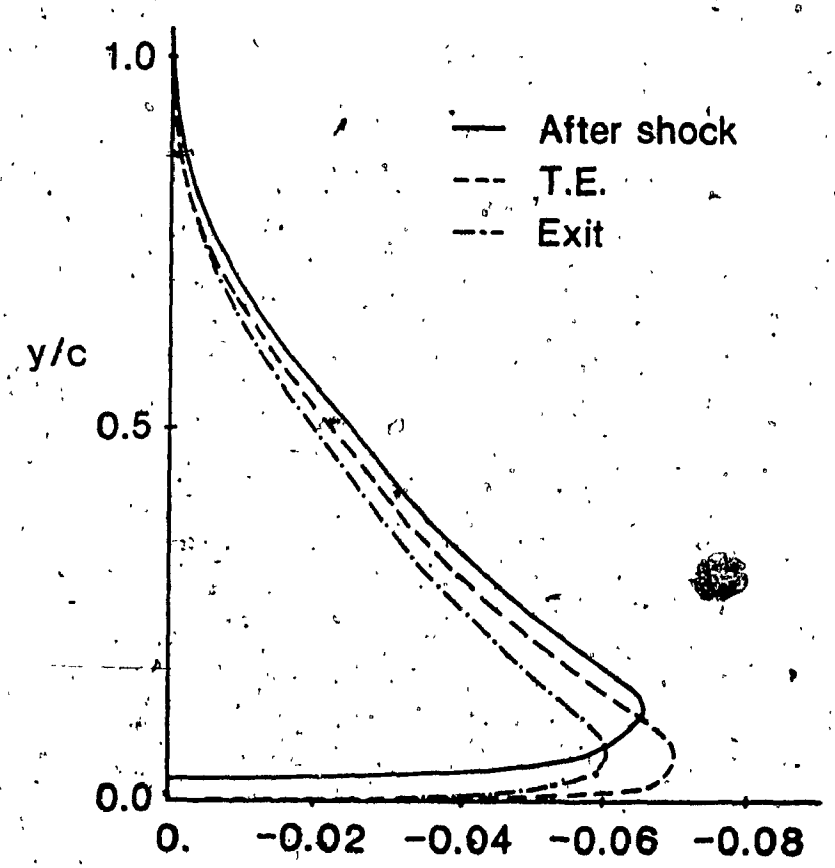

Fig. 4.14 Vorticity vs. Lateral Direction (M_∞=0.85)

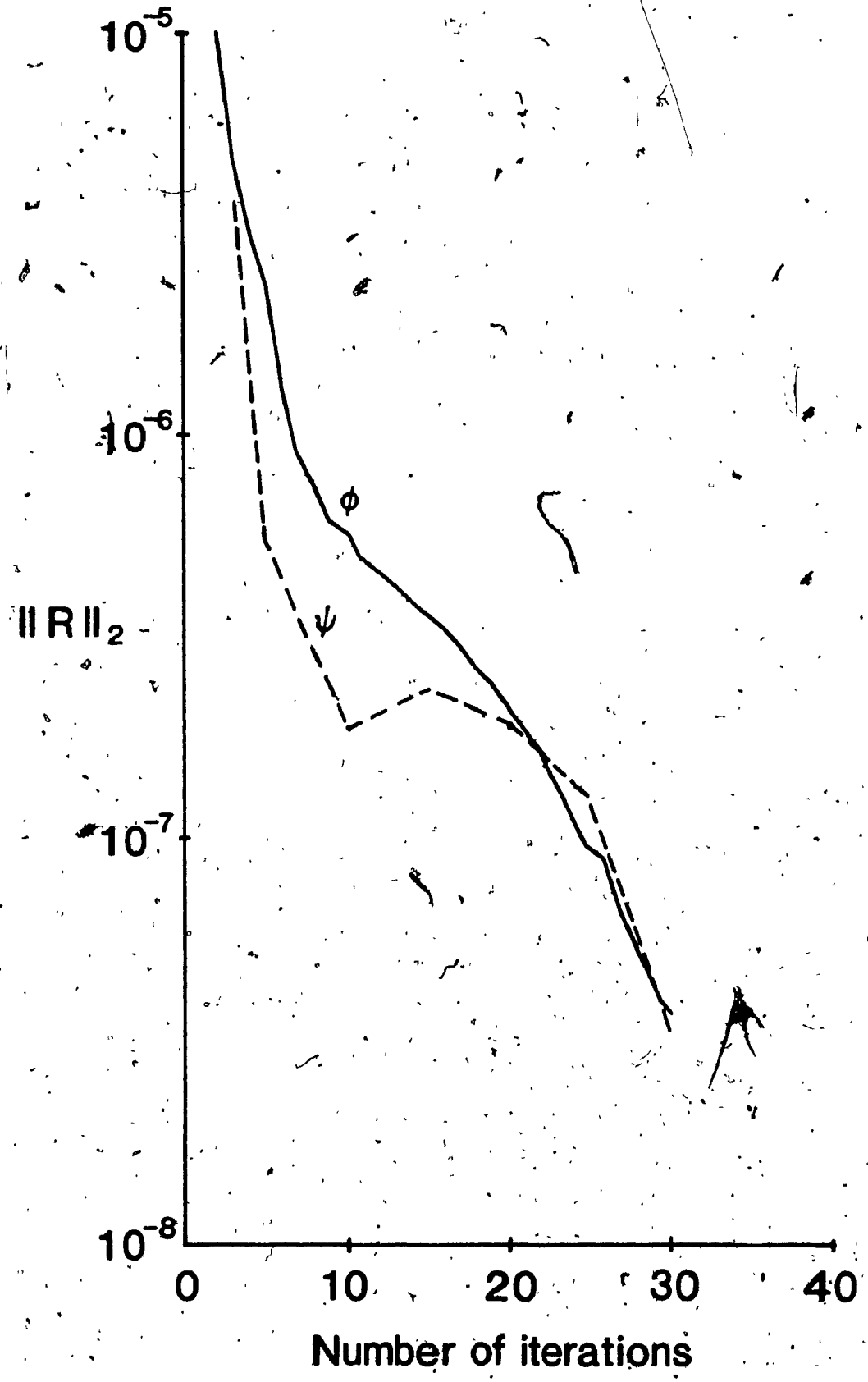

Fig. 4.15 Convergence History (M_∞=0.80)

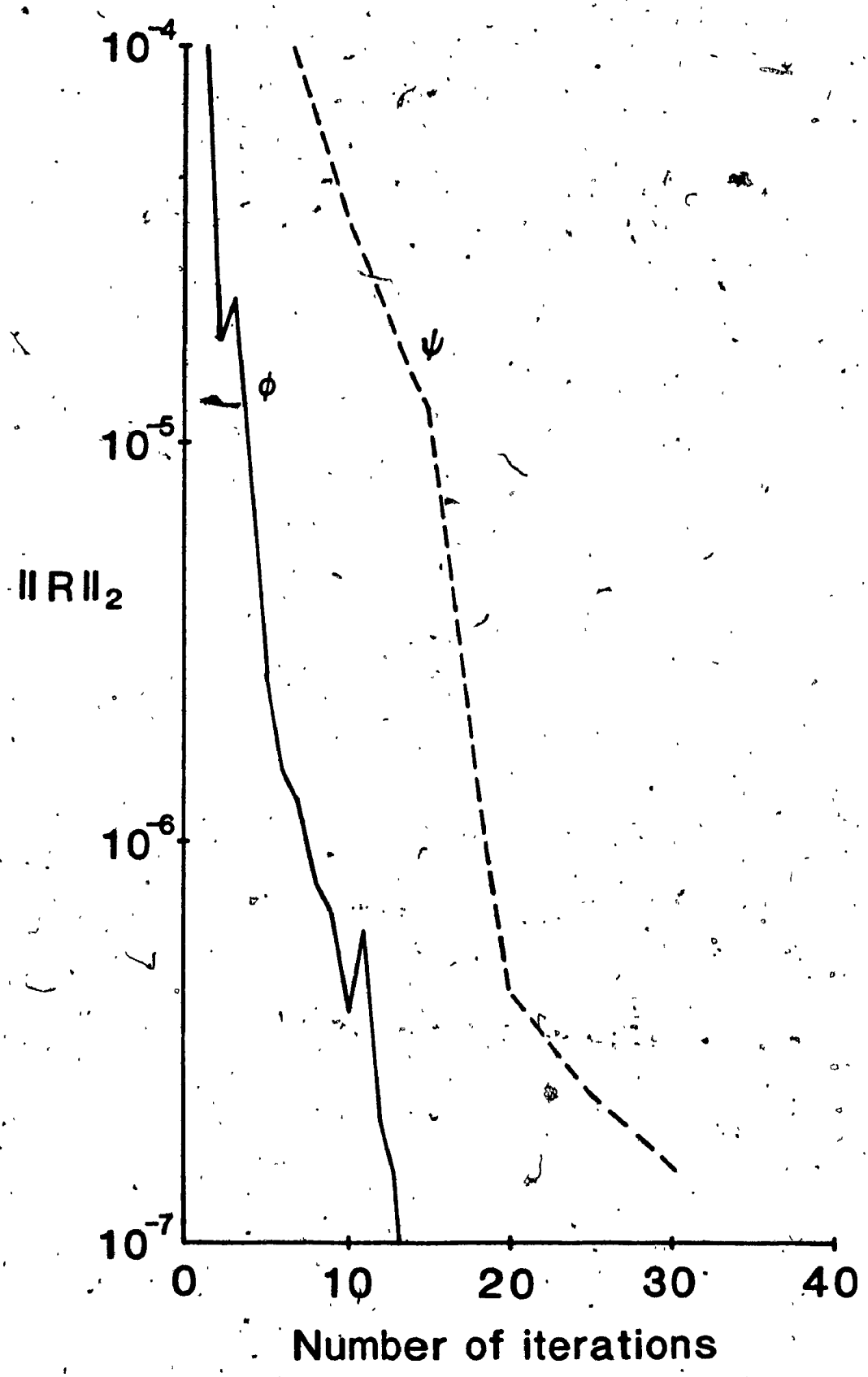

Fig. 4.16 Convergence History (M_∞=0.85)